COMPILED MODULE: GUYTON SPECIAL

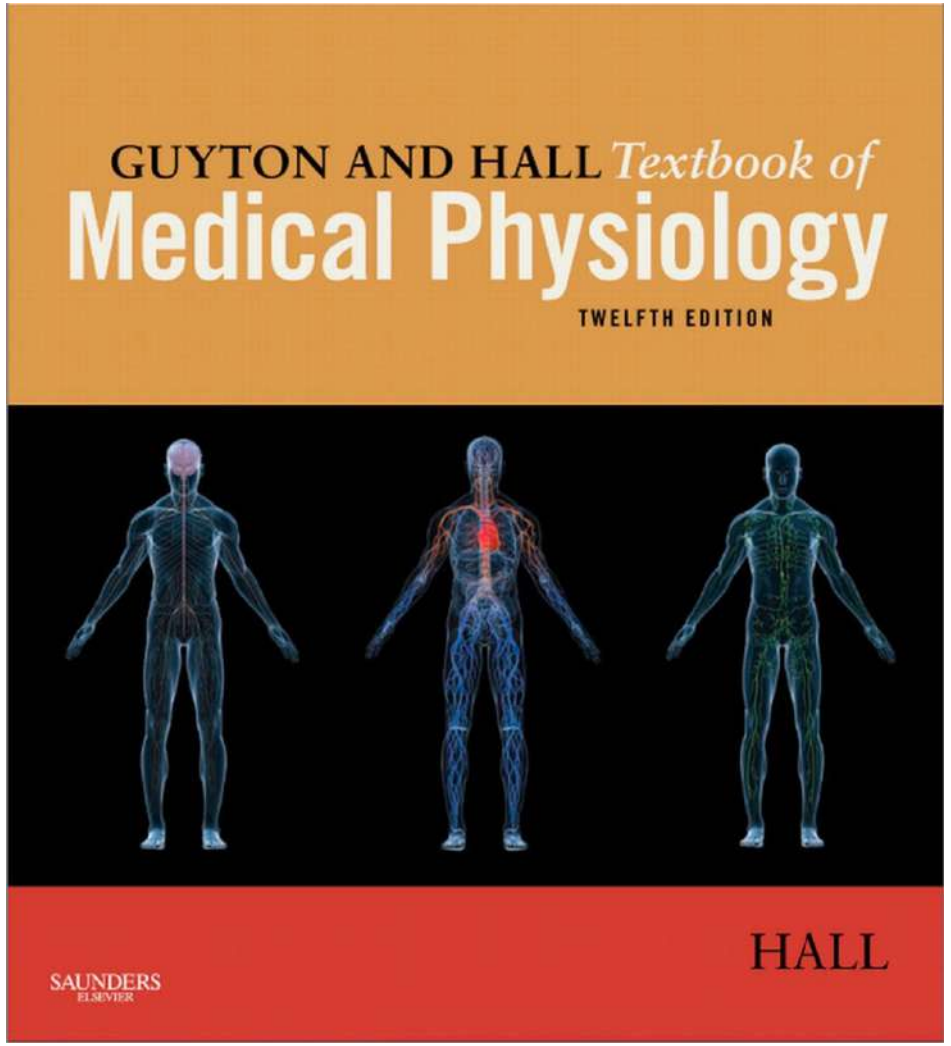

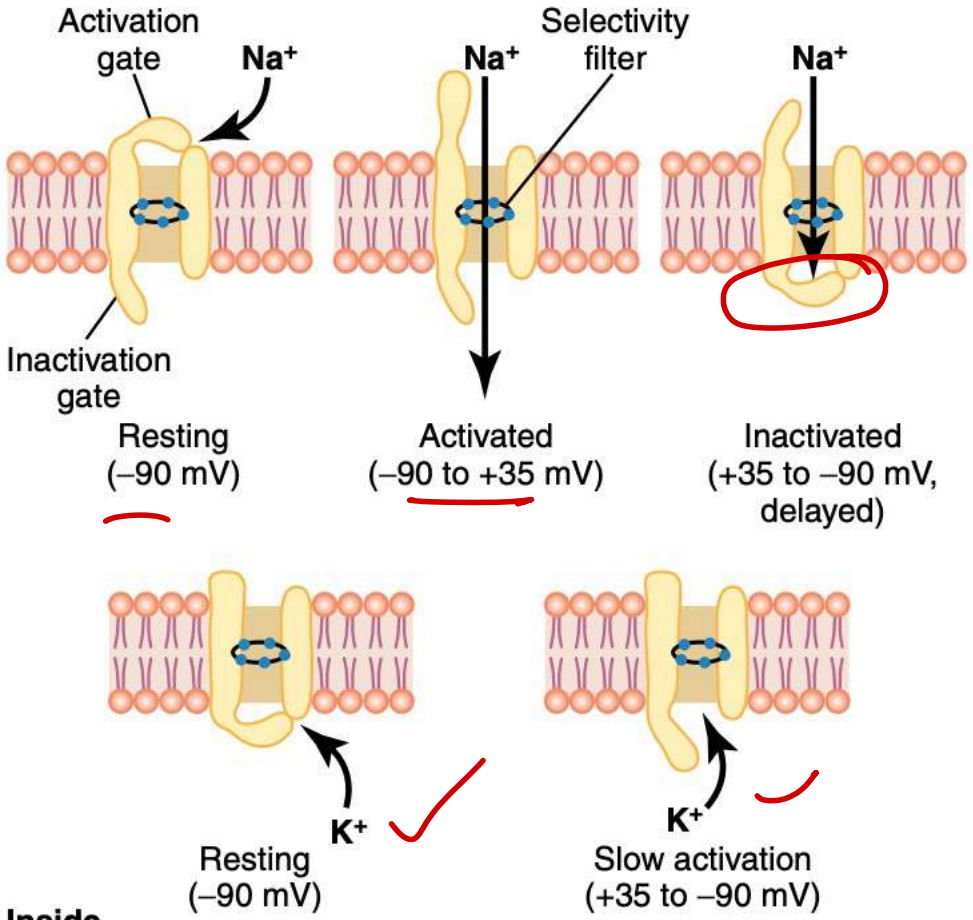

Figure 5-7 Characteristics of the voltage-gated sodium (*top*) and potassium (*bottom*) channels, showing successive activation and inactivation of the sodium channels and delayed activation of the potassium channels when the membrane potential is changed from the normal resting negative value to a positive value.

explosive development of an action potential. This level of –65 millivolts is said to be the *threshold* for stimulation.

ARP

Another important characteristic of the sodium channel inactivation process is that the inactivation gate will not reopen until the membrane potential returns to or near the original resting membrane potential level. Therefore, it is usually not possible for the sodium channels to open again without first repolarizing the nerve fiber.

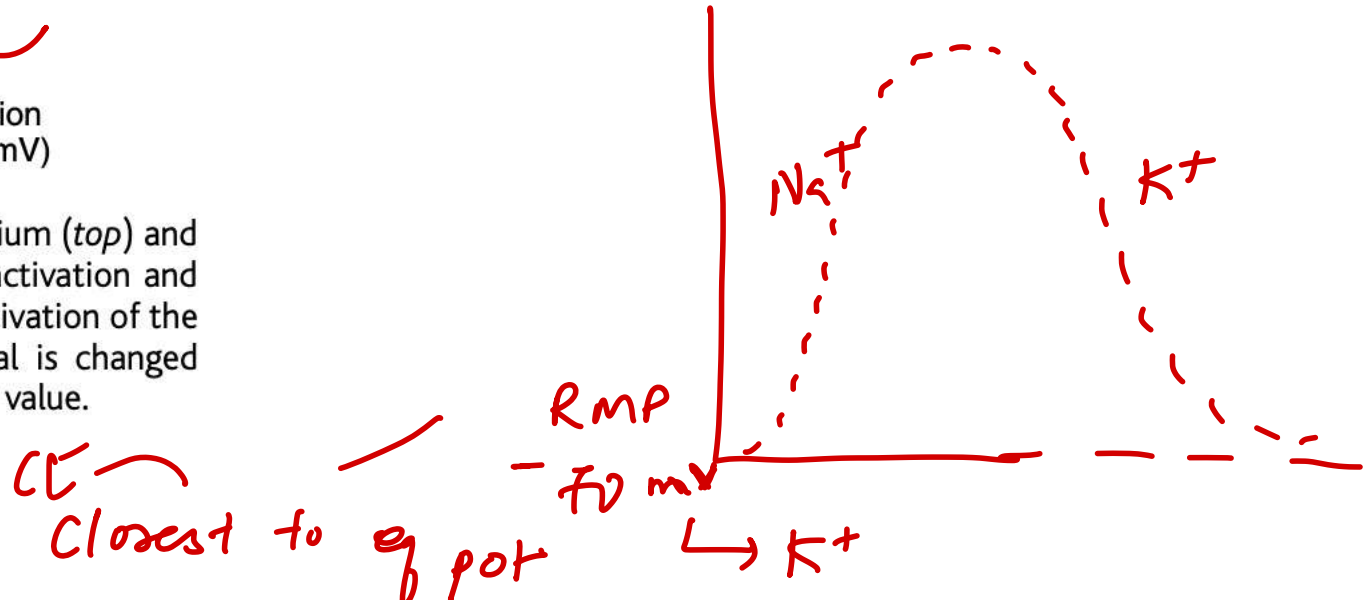

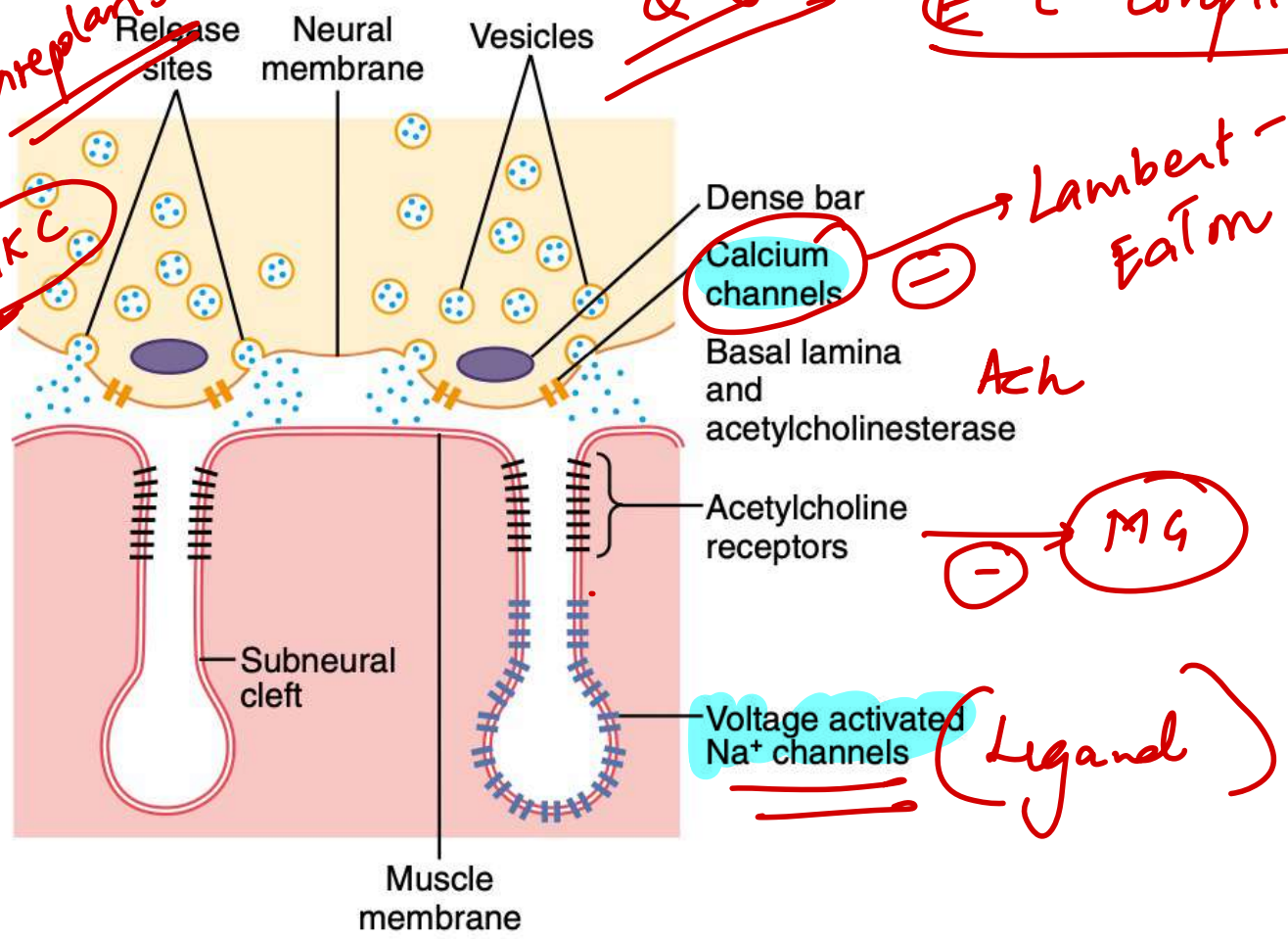

Figure 7-2 Release of acetylcholine from synaptic vesicles at the neural membrane of the neuromuscular junction. Note the proximity of the release sites in the neural membrane to the acetylcholine receptors in the muscle membrane, at the mouths of the subneural clefts.

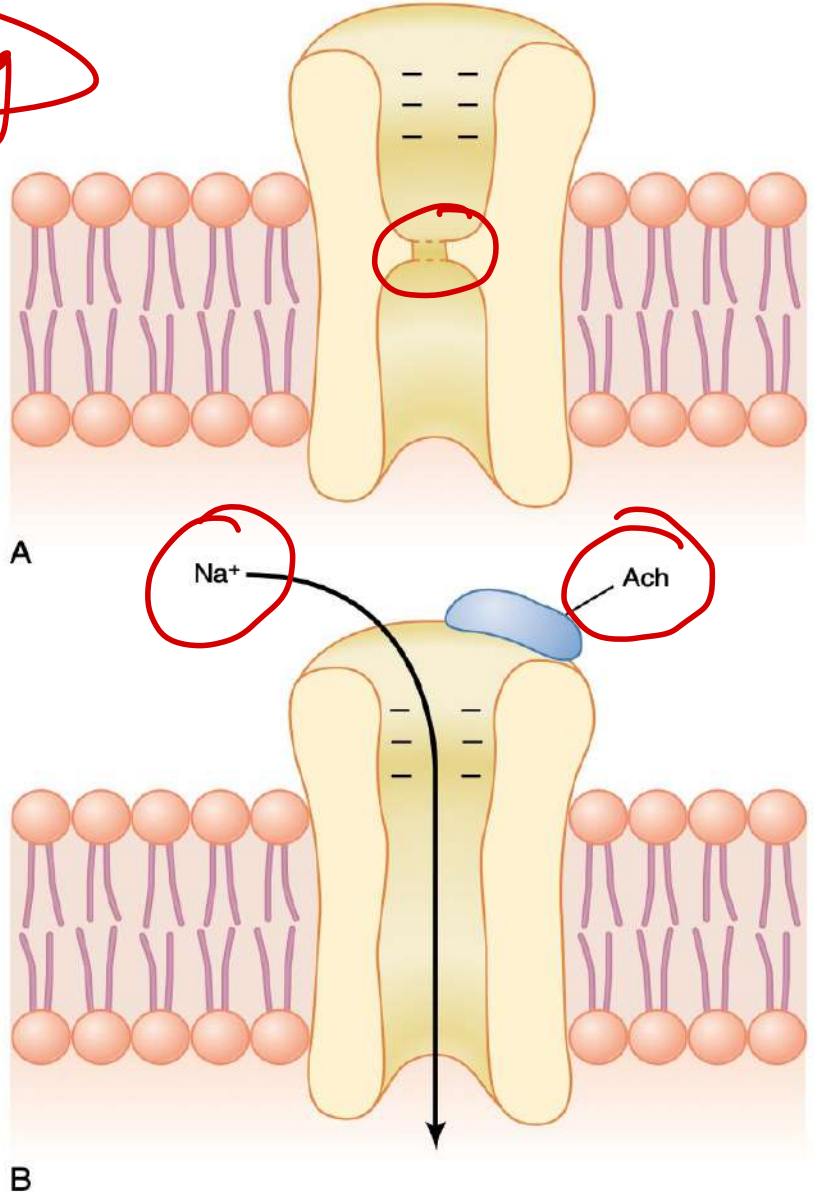

Figure 7-3 Acetylcholine-gated channel. *A*, Closed state. *B*, After acetylcholine (Ach) has become attached and a conformational change has opened the channel, allowing sodium ions to enter the muscle fiber and excite contraction. Note the negative charges at the channel mouth that prevent passage of negative ions such as chloride ions.

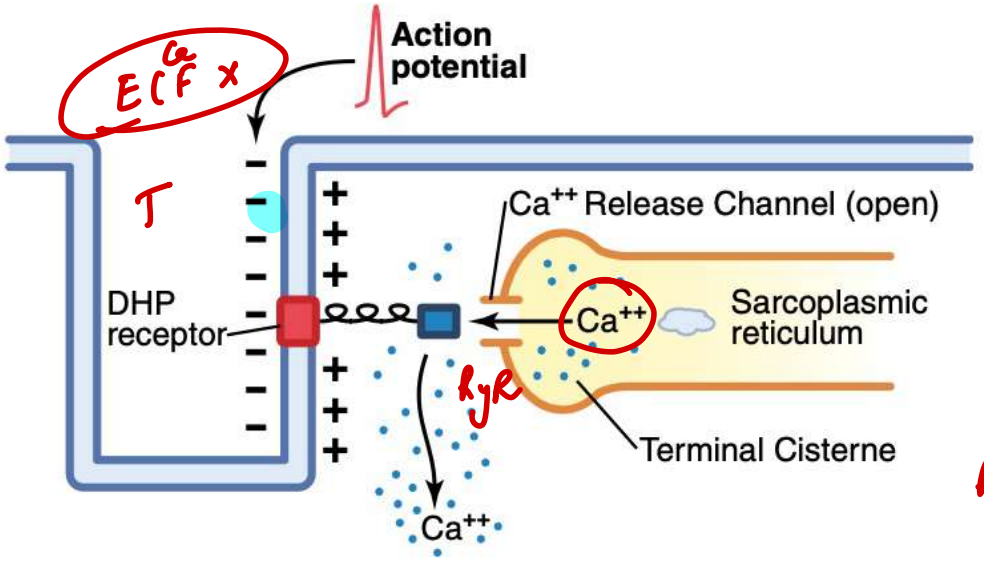

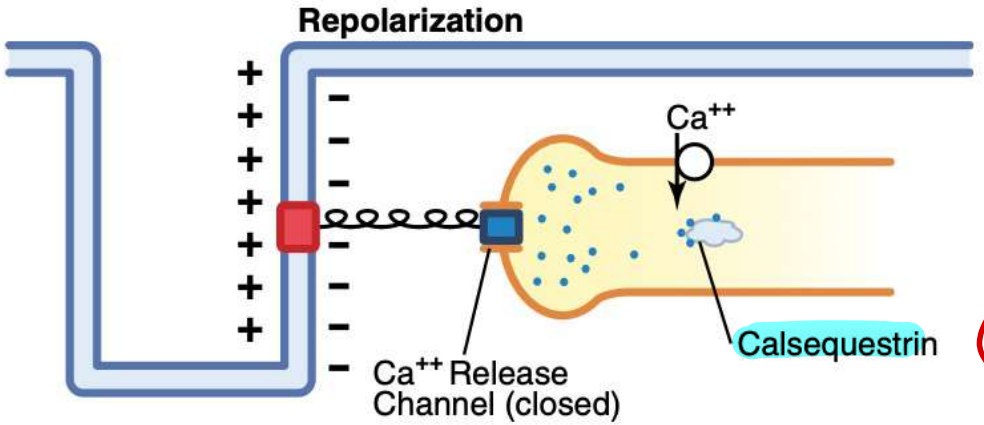

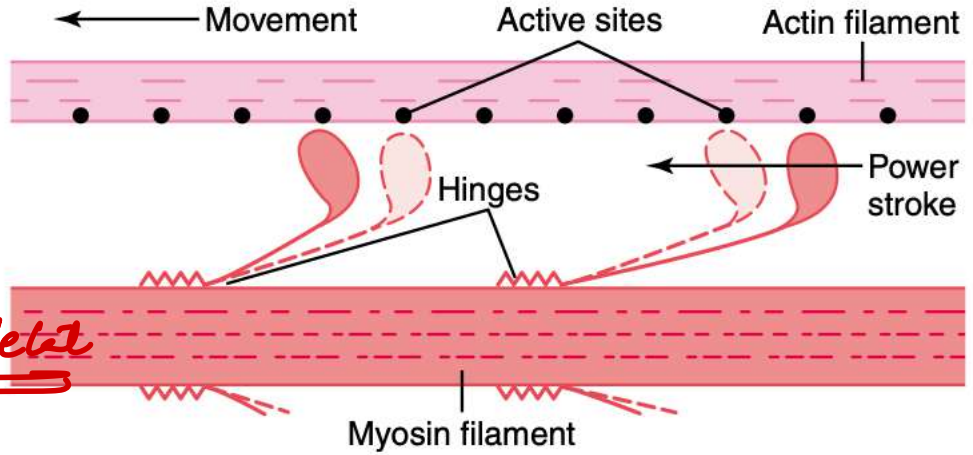

Figure 6-8 "Walk-along" mechanism for contraction of the muscle.

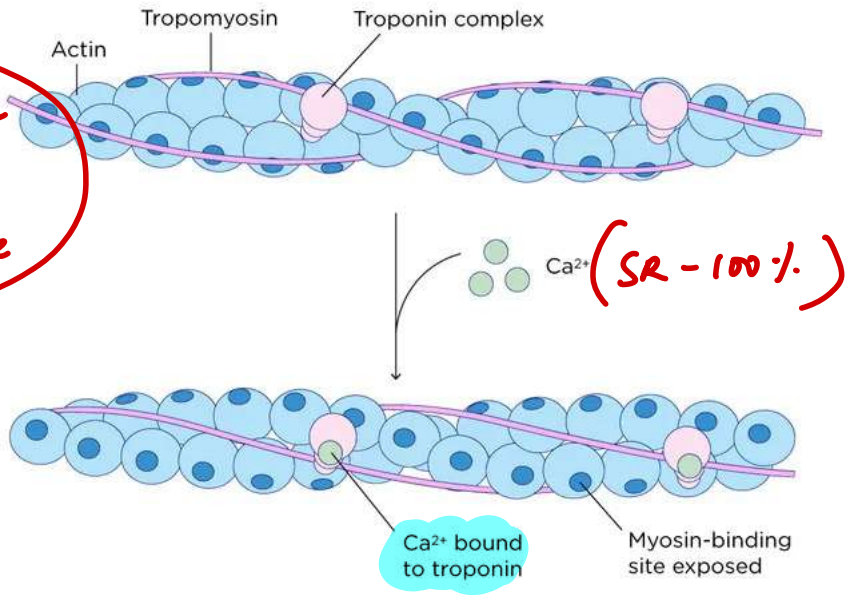

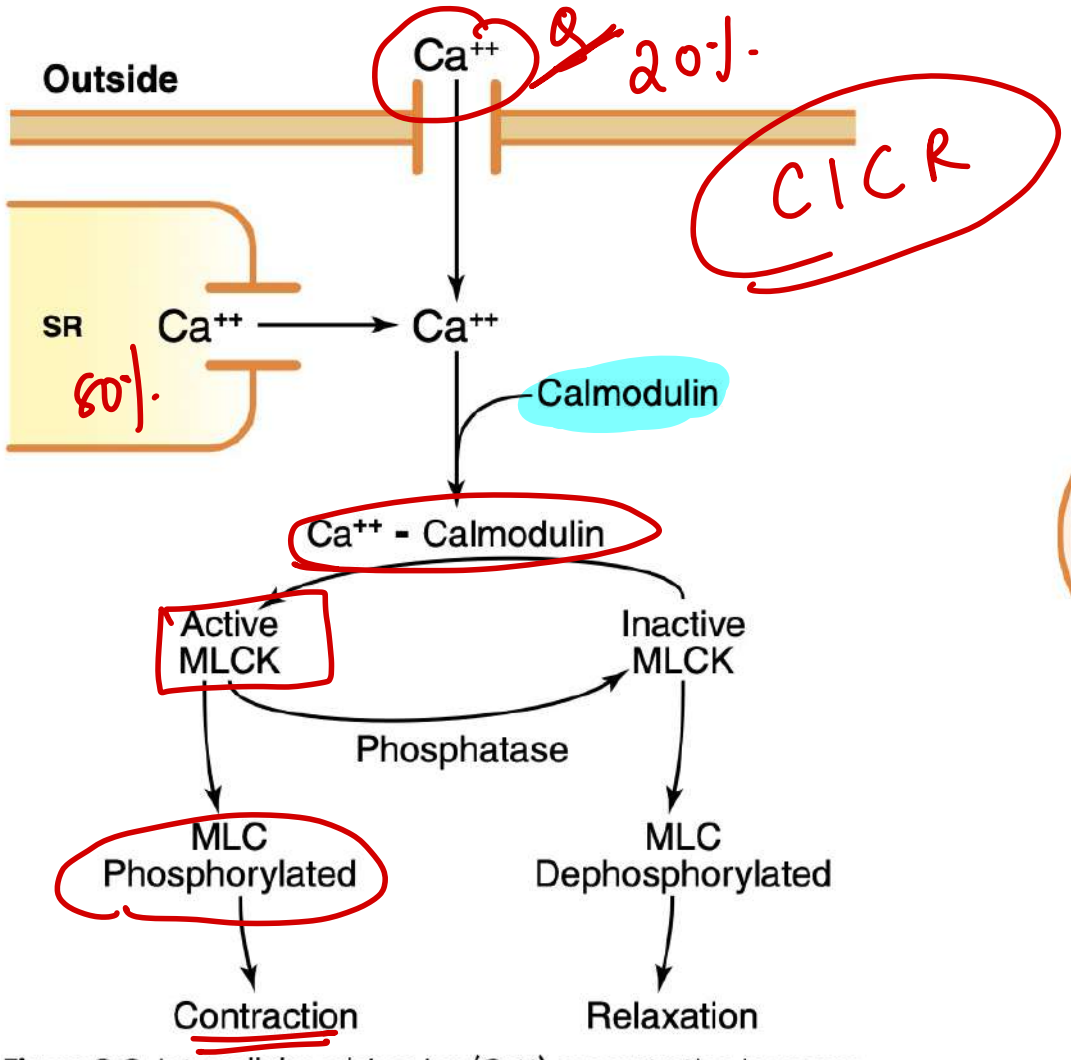

Figure 8-3 Intracellular calcium ion (Ca^{++}) concentration increases when Ca^{++} enters the cell through calcium channels in the cell membrane or the sarcoplasmic reticulum (SR). The Ca^{++} binds to calmodulin to form a Ca^{++}-calmodulin complex, which then activates myosin light chain kinase (MLCK). The MLCK phosphorylates the myosin light chain (MLC) leading to contraction of the smooth muscle. When Ca^{++} concentration decreases, due to pumping of Ca^{++} out of the cell, the process is reversed and myosin phosphatase removes the phosphate from MLC, leading to relaxation.

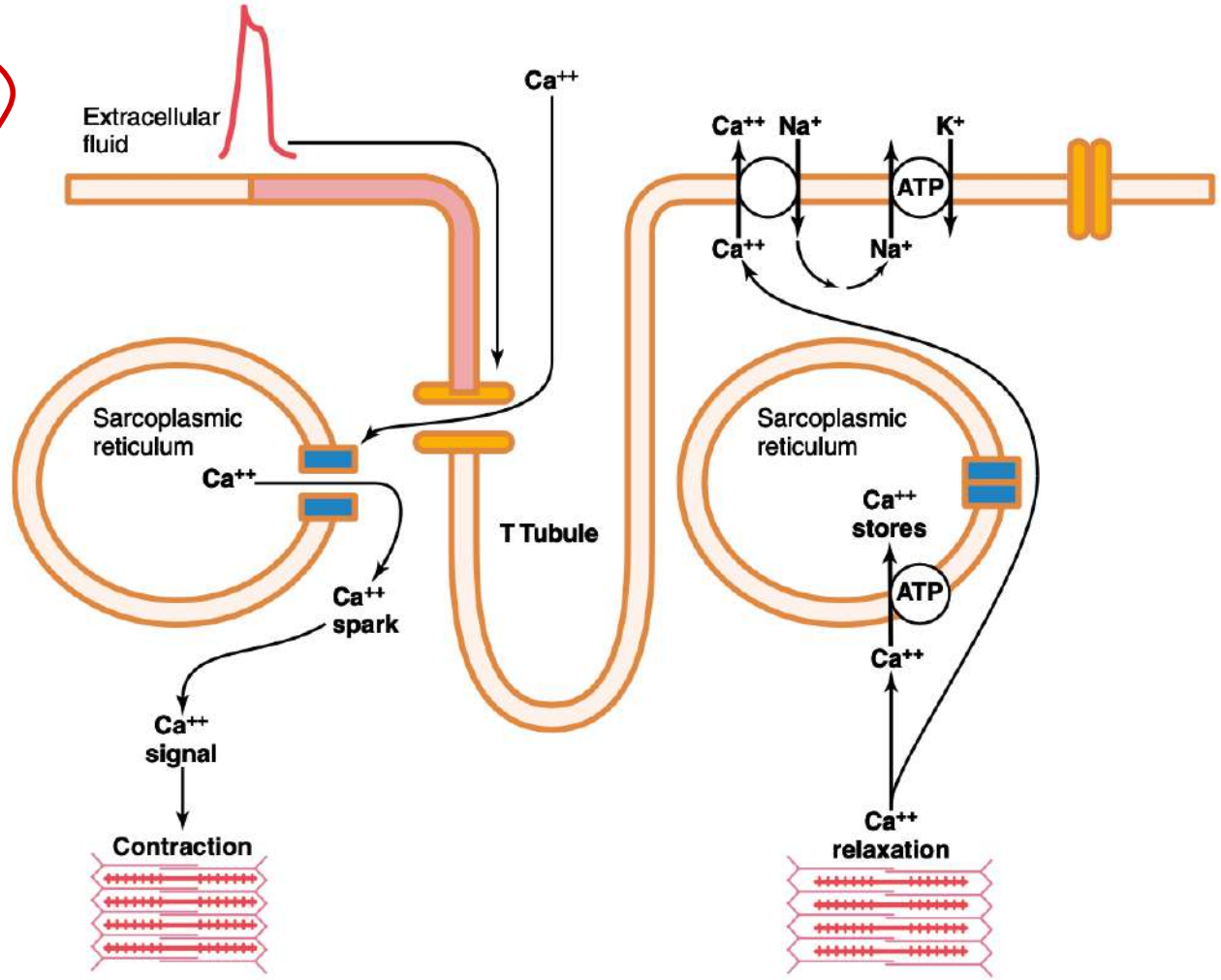

Figure 9-5 Mechanisms of excitation-contraction coupling and relaxation in cardiac muscle.

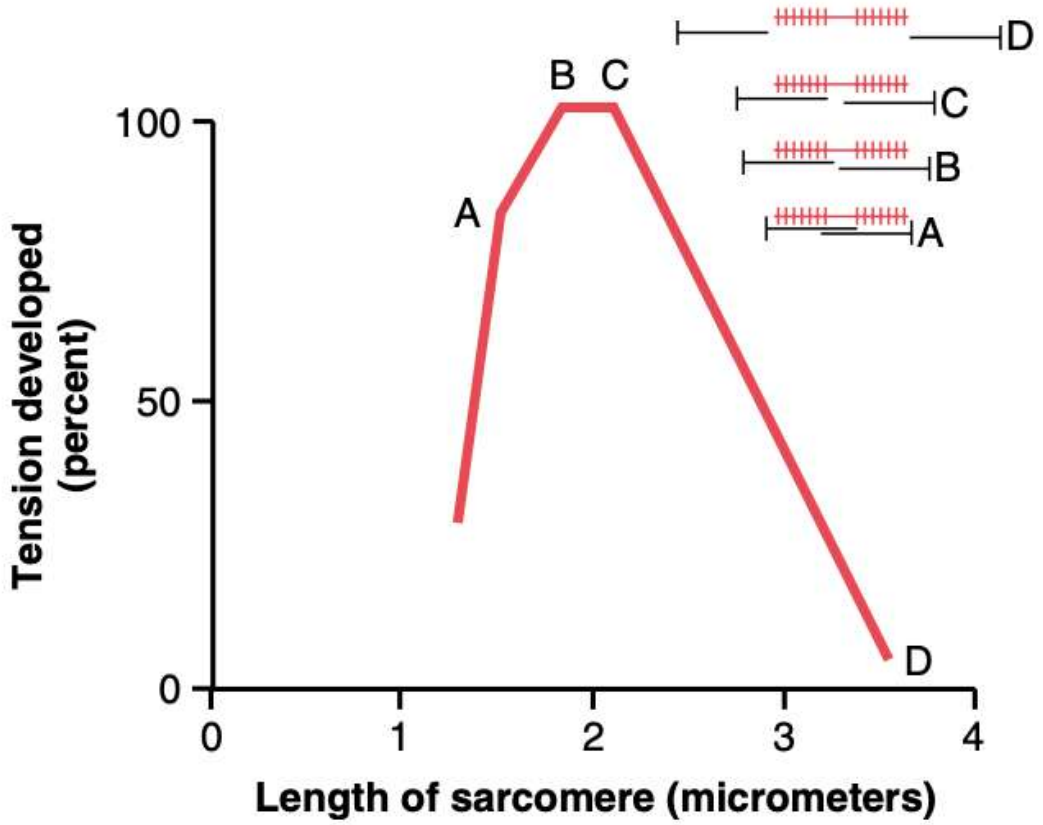

Figure 6-9 Length-tension diagram for a single fully contracted sarcomere, showing maximum strength of contraction when the sarcomere is 2.0 to 2.2 micrometers in length. At the upper right are the relative positions of the actin and myosin filaments at different sarcomere lengths from *point A* to *point D*. (Modified from Gordon AM, Huxley AF, Julian FJ: The length-tension diagram of single vertebrate striated muscle fibers. J Physiol 171:28P, 1964.)

optimal length

2 - 2.2 μ

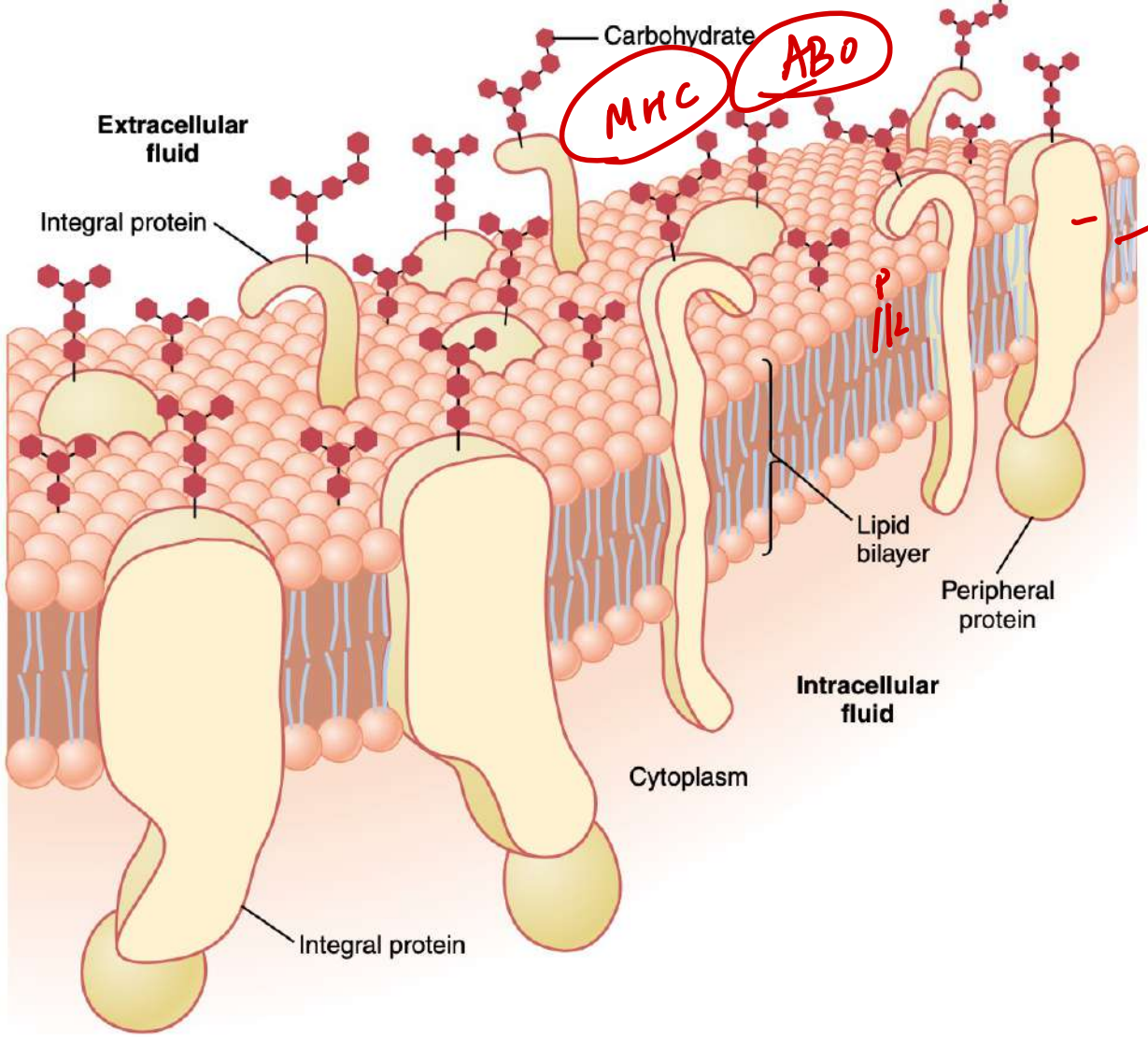

ure 2-3 Structure of the cell membrane, showing that it is composed mainly of a lipid bilayer of phospholipid molecules, but with large nbers of protein molecules protruding through the layer. Also, carbohydrate moieties are attached to the protein molecules on the out- of the membrane and to additional protein molecules on the inside. (Redrawn from Lodish HF, Rothman JE: The assembly of cell mem-

Cell Membrane

The cell membrane (also called the *plasma membrane*), which envelops the cell, is a thin, pliable, elastic structure only 7.5 to 10 nanometers thick. It is composed almost entirely of proteins and lipids. The approximate composition is proteins, 55 percent; phospholipids, 25 percent; cholesterol, 13 percent; other lipids, 4 percent; and carbohydrates, 3 percent.

	EXTRACELLULAR FLUID	INTRACELLULAR FLUID
Na^+	142 mEq/L	10 mEq/L
K^+	4 mEq/L	140 mEq/L
Ca^{++}	2.4 mEq/L	0.0001 mEq/L
Mg^{++}	1.2 mEq/L	58 mEq/L
Cl^-	103 mEq/L	4 mEq/L
HCO_3^-	28 mEq/L	10 mEq/L
Phosphates	4 mEq/L	75 mEq/L
$SO_4^=$	1 mEq/L	2 mEq/L
Glucose	90 mg/dl	0 to 20 mg/dl
Amino acids	30 mg/dl	200 mg/dl ?
Cholesterol, Phospholipids, Neutral fat	0.5 g/dl	2 to 95 g/dl
PO_2	35 mm Hg	20 mm Hg ?
PCO_2	46 mm Hg	50 mm Hg ?
pH	7.4	7.0
Proteins	2 g/dl (5 mEq/L)	16 g/dl (40 mEq/L)

KMP

Refeeding Sx

Tumor lysis

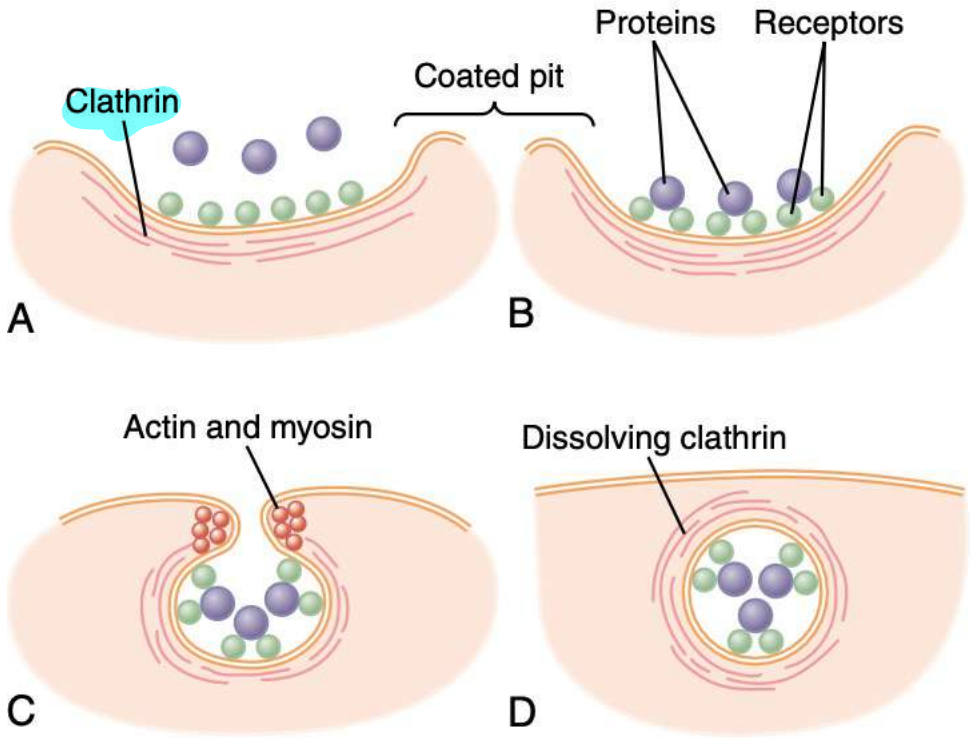

Figure 2-11 Mechanism of pinocytosis.

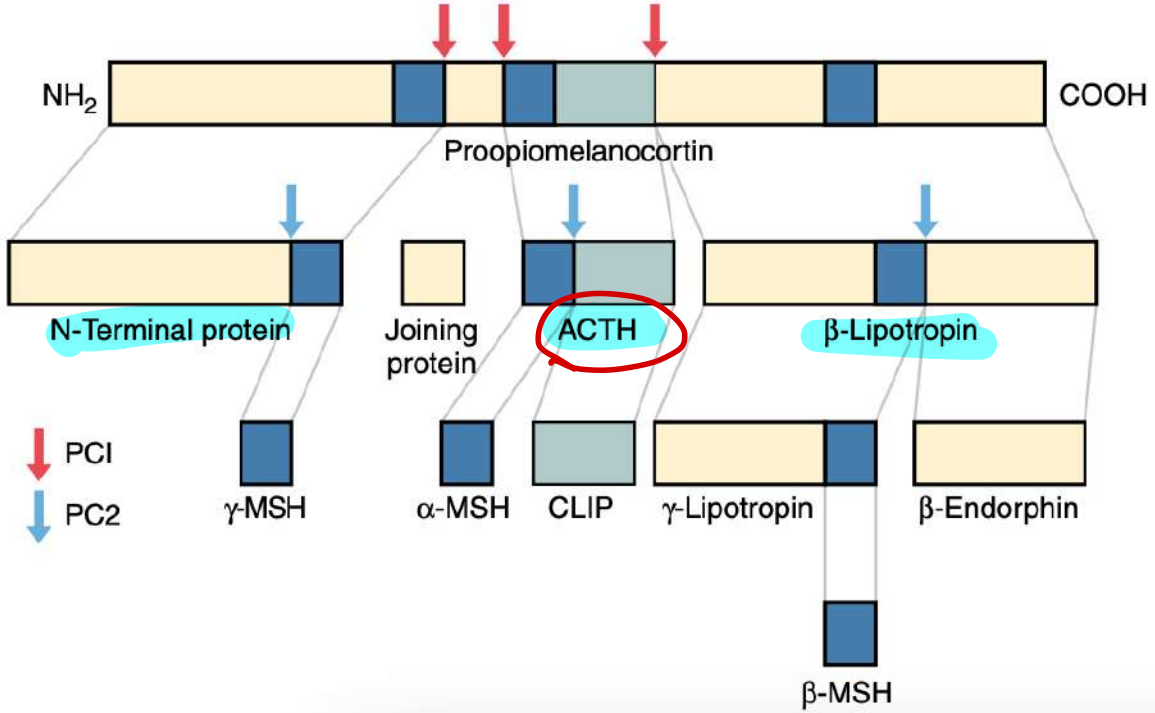

Figure 77-9 Proopiomelanocortin (POMC) processing by prohormone convertase 1 (PC1, *red arrows*) and PC 2 (*blue arrows*). Tissue-specific expression of these two enzymes results in different peptides produced in various tissues. The anterior pituitary expresses PC1, resulting in formation of N-terminal peptide, joining peptide, ACTH, and β-lipotropin. Expression of PC2 within the hypothalamus leads to the production of α-, β-, and γ-melanocyte stimulating hormone (MSH), but not ACTH. CLIP, corticotropin-like intermediate peptide.

1° adrenal insuff

↑CRH → ↑ACTH

↑MSH

Pigmentn

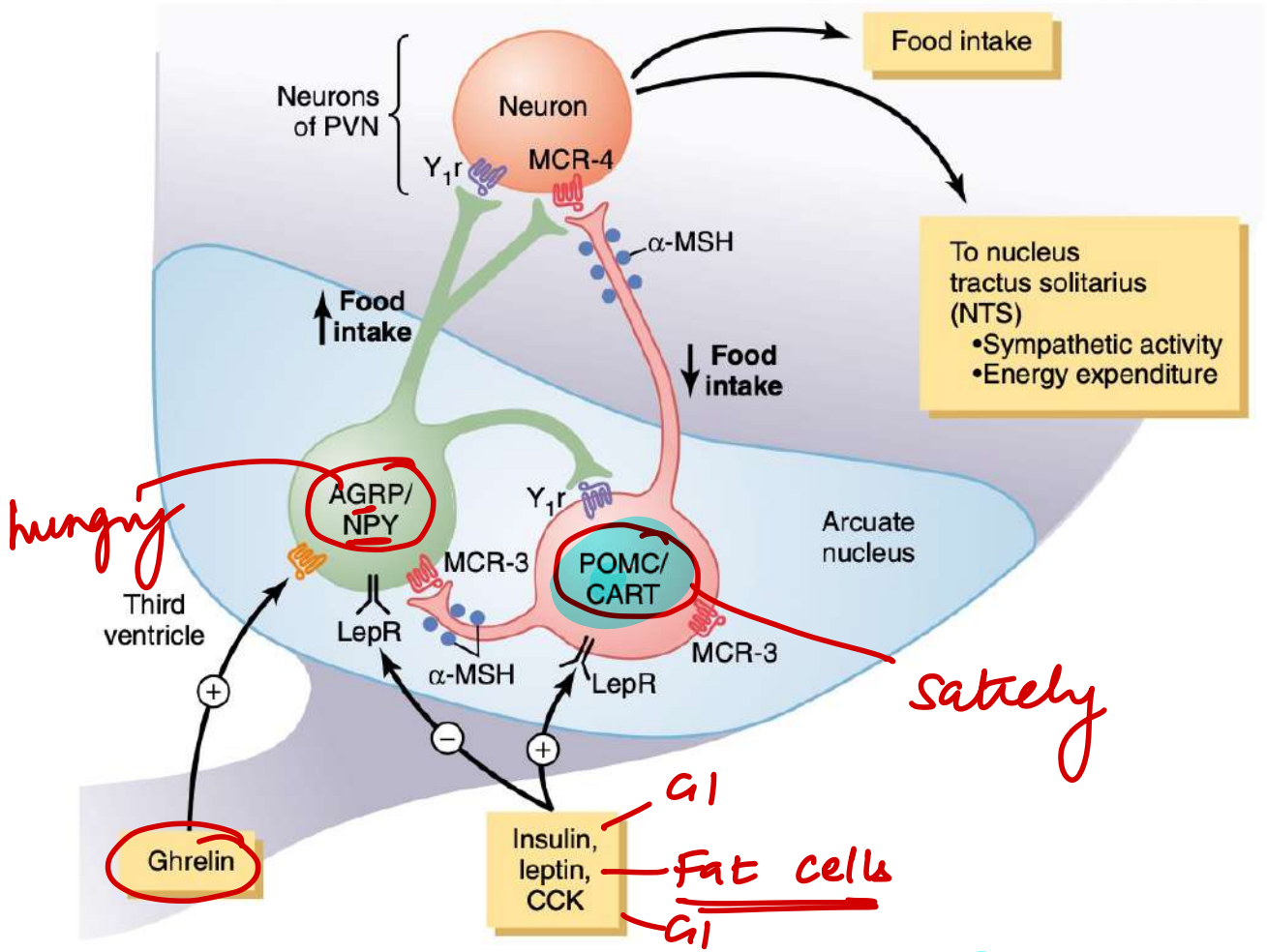

Decrease Feeding (Anorexigenic)	Increase Feeding (Orexigenic)
α-Melanocyte-stimulating hormone (α-MSH)	Neuropeptide Y (NPY)
Leptin	Agouti-related protein (AGRP)
Serotonin	Melanin-concentrating hormone (MCH)
Norepinephrine	Orexins A and B
Corticotropin-releasing hormone	Endorphins
Insulin	Galanin (GAL)
Cholecystokinin (CCK)	Amino acids (glutamate and γ-aminobutyric acid)
Glucagon-like peptide (GLP)	Cortisol
Cocaine- and amphetamine-regulated transcript (CART)	Ghrelin
Peptide YY (PYY)	Endocannabinoids

Figure 71-2 Control of energy balance by two types of neurons of the arcuate nuclei: (1) pro-opiomelanocortin (*POMC*) neurons that release α-melanocyte-stimulating hormone (*α-MSH*) and cocaine- and amphetamine-regulated transcript (*CART*), decreasing food intake and increasing energy expenditure and (2) neurons that produce agouti-related protein (*AGRP*) and neuropeptide Y (*NPY*), increasing food intake and reducing energy expenditure. α-MSH released by POMC neurons stimulates melanocortin receptors (*MCR-3* and *MCR-4*) in the paraventricular nuclei (*PVN*), which then activate neuronal pathways that project to the nucleus tractus solitarius (*NTS*) and increase sympathetic activity and energy expenditure. AGRP acts as an antagonist of MCR-4. Insulin, leptin, and cholecystokinin (*CCK*) are hormones that inhibit AGRP-NPY neurons and stimulate adjacent POMC-CART neurons, thereby reducing food intake. Ghrelin, a hormone secreted from the stomach, activates AGRP-NPY neurons and stimulates food intake. LepR, leptin receptor; Y_1R, neuropeptide Y1 receptor. (Redrawn from Barsh GS, Schwartz MW: Nature Rev Genetics 3:589, 2002.)

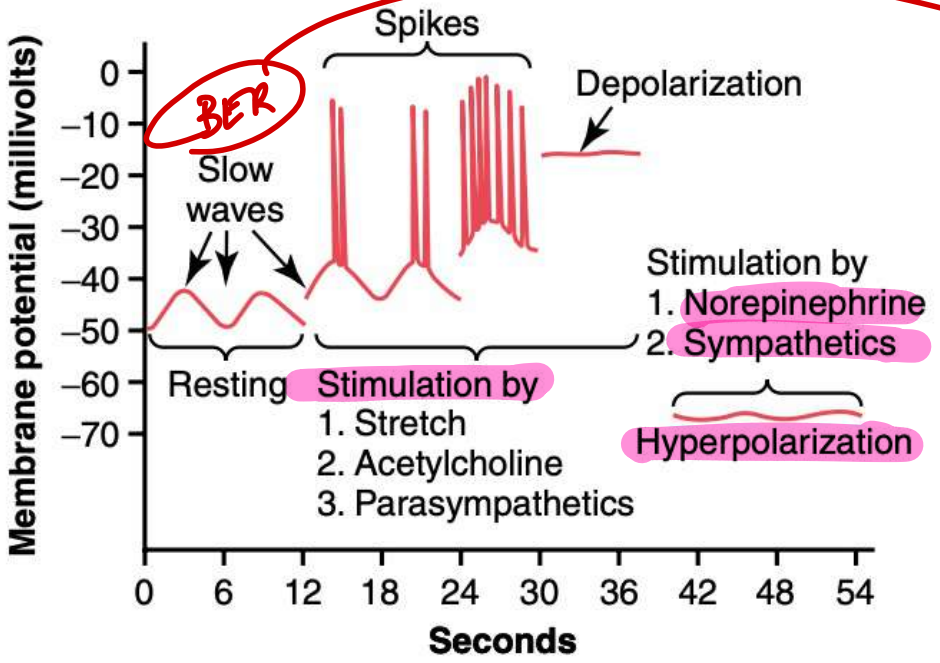

Figure 62-3 Membrane potentials in intestinal smooth muscle. Note the slow waves, the spike potentials, total depolarization, and hyperpolarization, all of which occur under different physiologic conditions of the intestine.

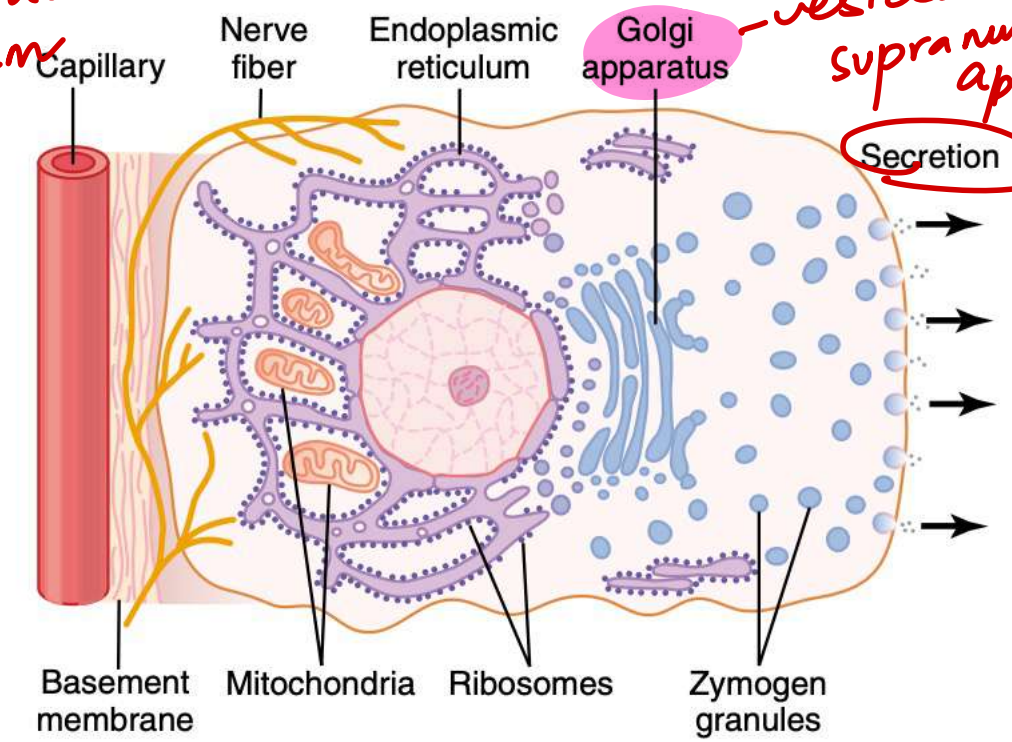

Figure 64-1 Typical function of a glandular cell for formation and secretion of enzymes and other secretory substances.

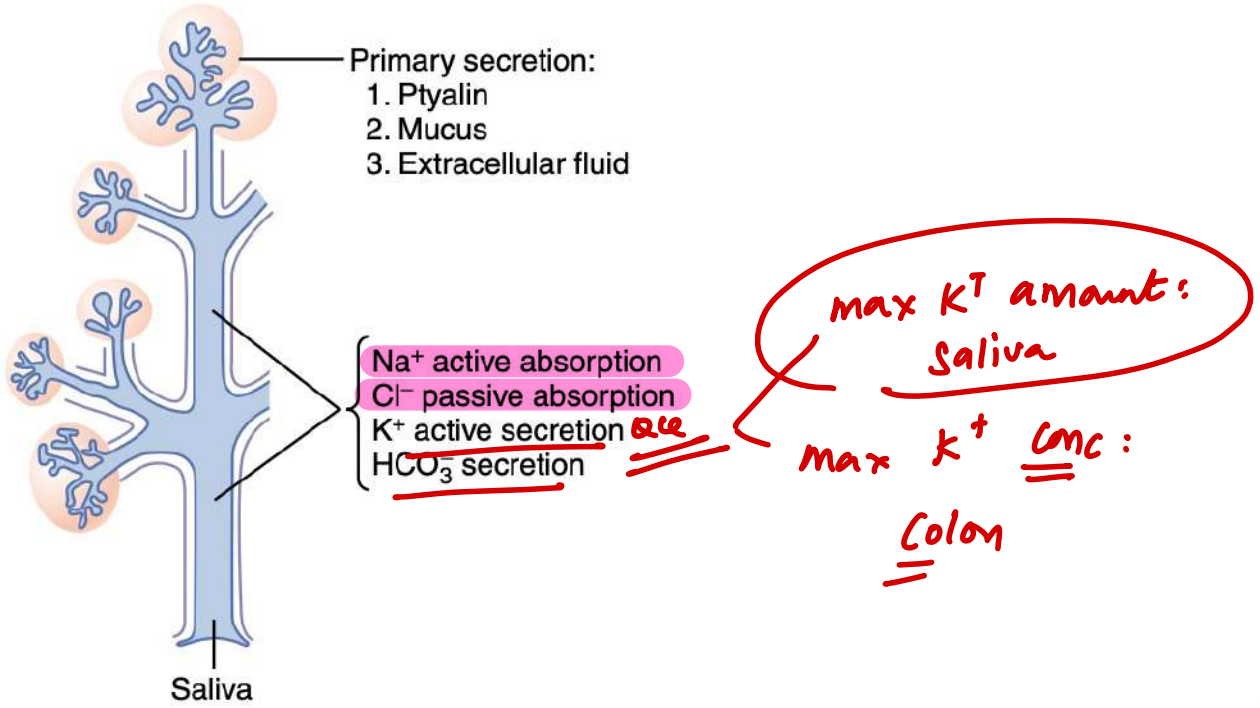

Figure 64-2 Formation and secretion of saliva by a submandibular salivary gland.

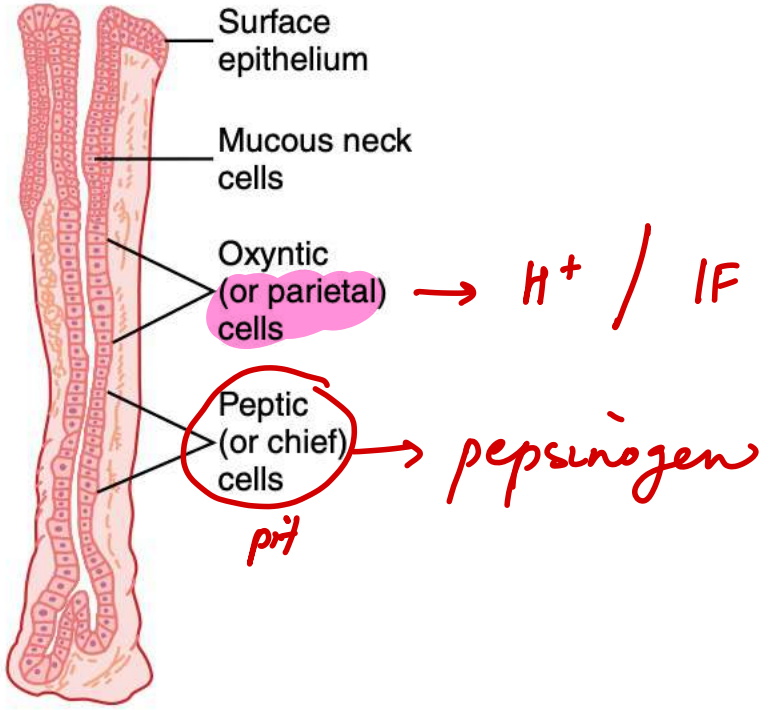

Figure 64-4 Oxyntic gland from the body of the stomach.

	Daily Volume (ml)	pH
Saliva	1000	6.0-7.0
Gastric secretion	1500	1.0-3.5
Pancreatic secretion	1000	8.0-8.3
Bile	1000	7.8
Small intestine secretion	1800	7.5-8.0
Brunner's gland secretion	200	8.0-8.9
Large intestinal secretion	200	7.5-8.0
Total	6700	

Conversely, the concentration of potassium ions is about 30 mEq/L, seven times as great as in plasma, and the concentration of bicarbonate ions is 50 to 70 mEq/L, about two to three times that of plasma.

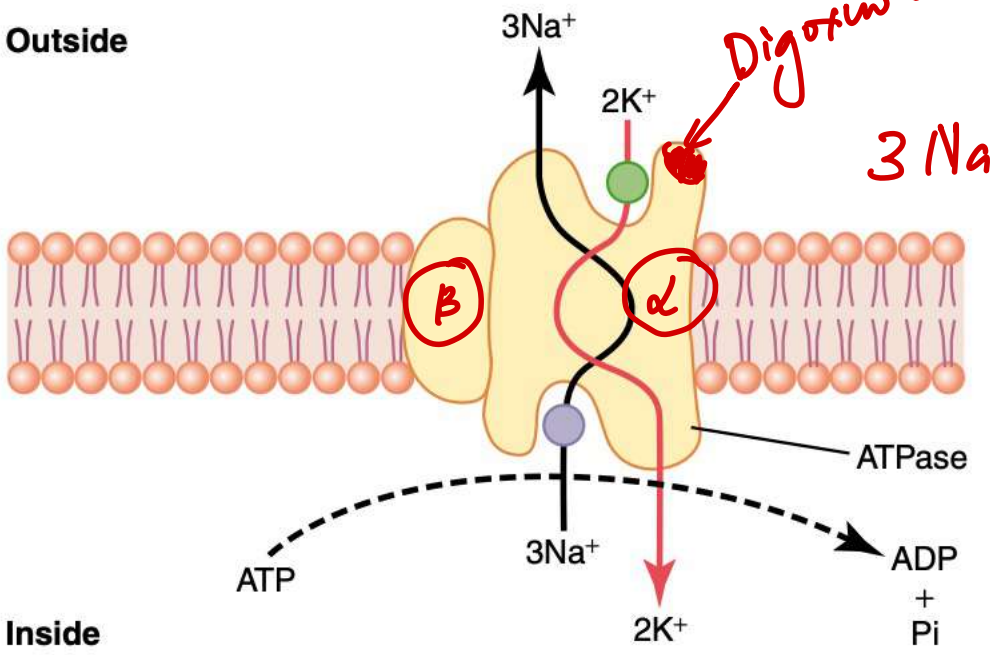

Digoxin bind

NO KIA

3 Na out K in 2

Na-K pump

Proton

SERCA

Primary Active Transport and Secondary Active Transport. Active transport is divided into two types according to the source of the energy used to cause the transport: *primary active transport* and *secondary active transport*. In primary active transport, the energy is derived directly from breakdown of adenosine triphosphate (ATP) or of some other high-energy phosphate compound. In secondary active transport, the energy is derived secondarily from energy that has been stored in the form of ionic concentration differences of secondary molecular or ionic substances between the two sides of a cell membrane, created originally by primary active transport. In both instances, transport depends on *carrier*

SGLT

Na - I symport

Coupling ratio : 3:2

outside the cell but leaves a deficit of positive ions inside the cell; that is, it causes negativity on the inside. Therefore, the Na^+-K^+ pump is said to be *electrogenic* because it creates an electrical potential across the cell membrane. As discussed in Chapter 5, this electrical potential is a basic requirement in nerve and muscle fibers for transmitting nerve and muscle signals.

↑Na-K+ ATP

Thyroxine

Insulin

aldesterone

Catecholamine

BMR

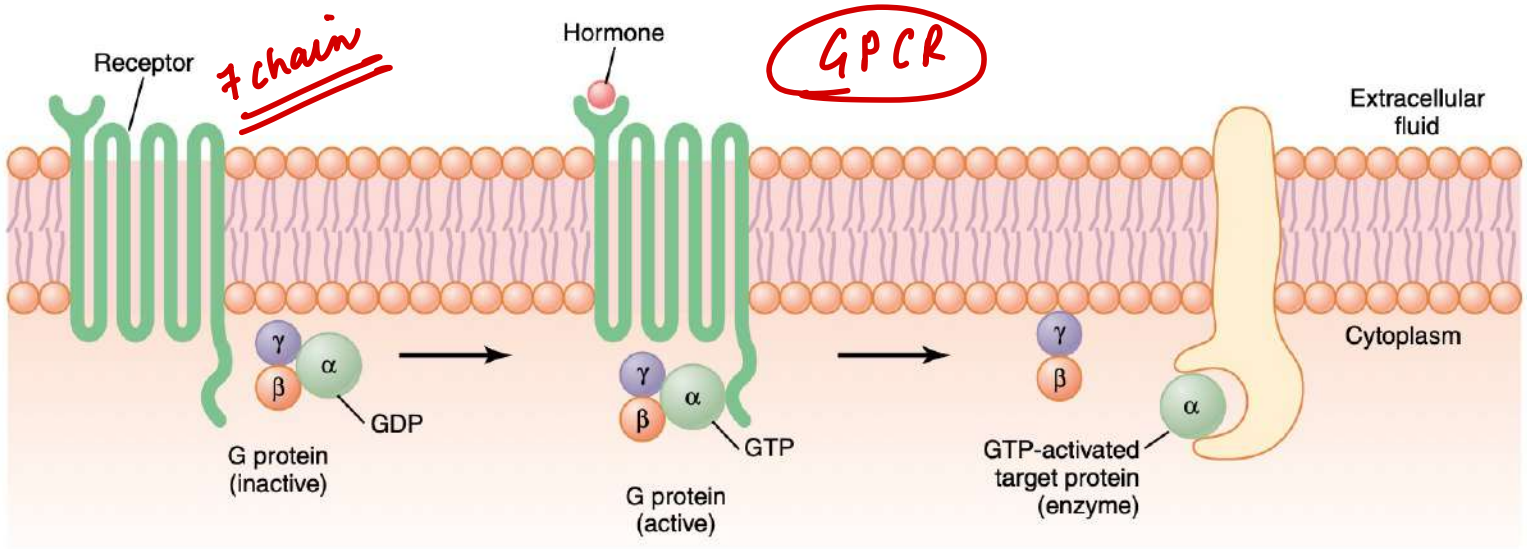

Figure 74-4 Mechanism of activation of a G protein–coupled receptor. When the hormone activates the receptor, the inactive α, β, and γ G protein complex associates with the receptor and is activated, with an exchange of guanosine triphosphate (GTP) for guanosine diphosphate (GDP). This causes the α subunit (to which the GTP is bound) to dissociate from the β and γ subunits of the G protein and to interact with membrane-bound target proteins (enzymes) that initiate intracellular signals.

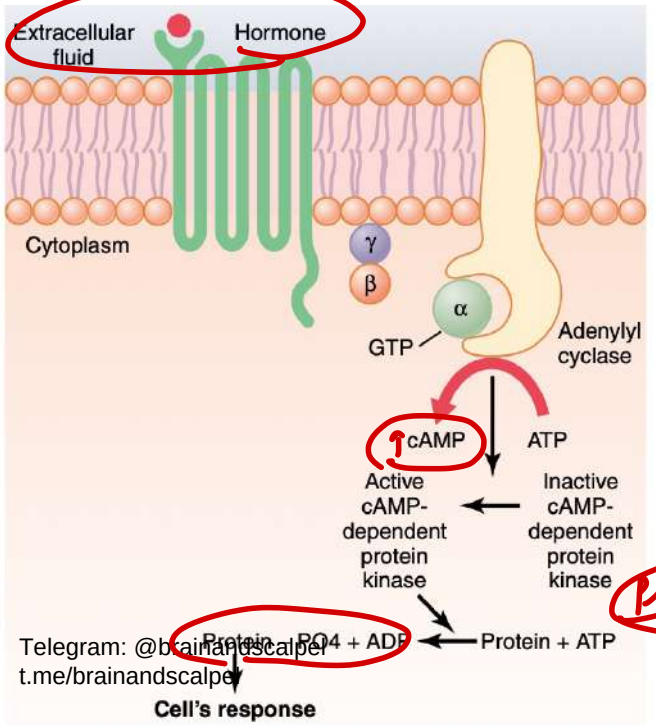

Gs ↑ cAMP

Gi ↓

Pkn k A ↑

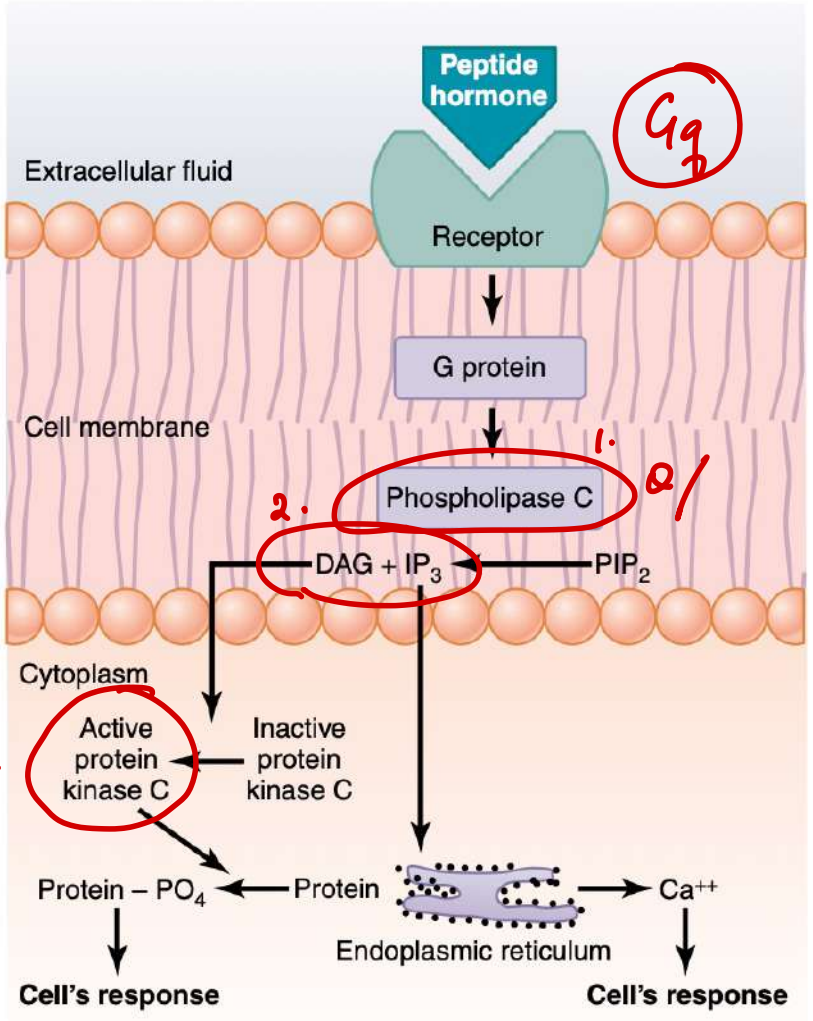

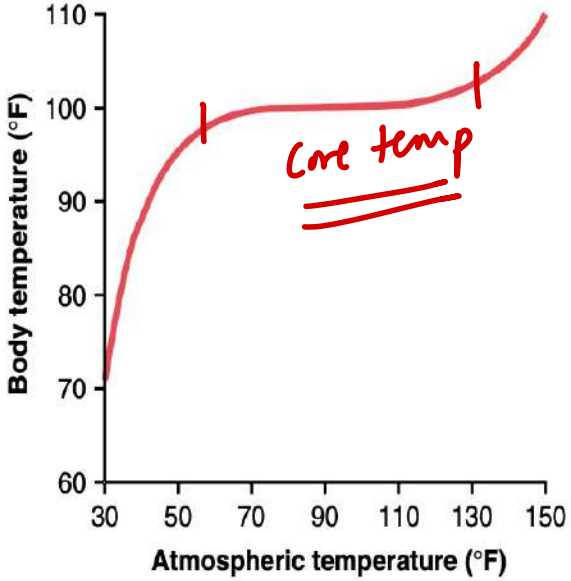

Figure 73-6 Effect of high and low atmospheric temperatures of several hours' duration, under dry conditions, on the internal body "core" temperature. Note that the internal body temperature remains stable despite wide changes in atmospheric temperature.

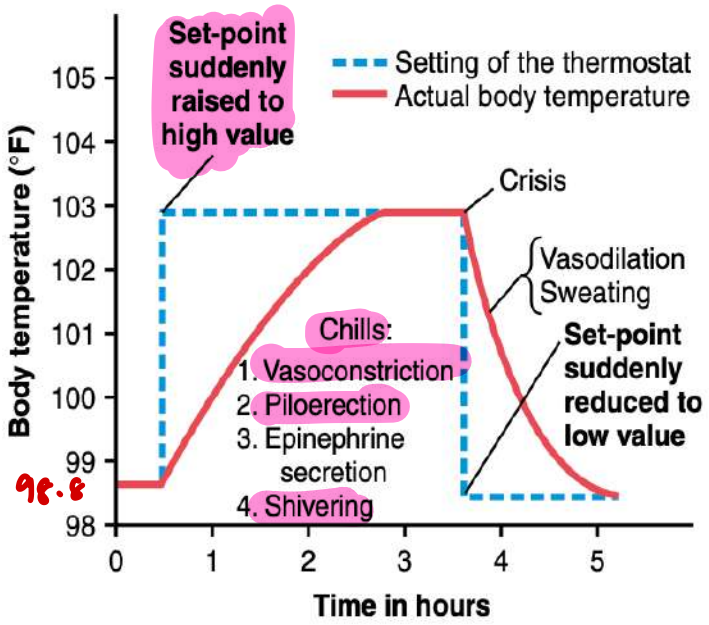

Figure 73-11 Effects of changing the set-point of the hypothalamic temperature controller.

QQ

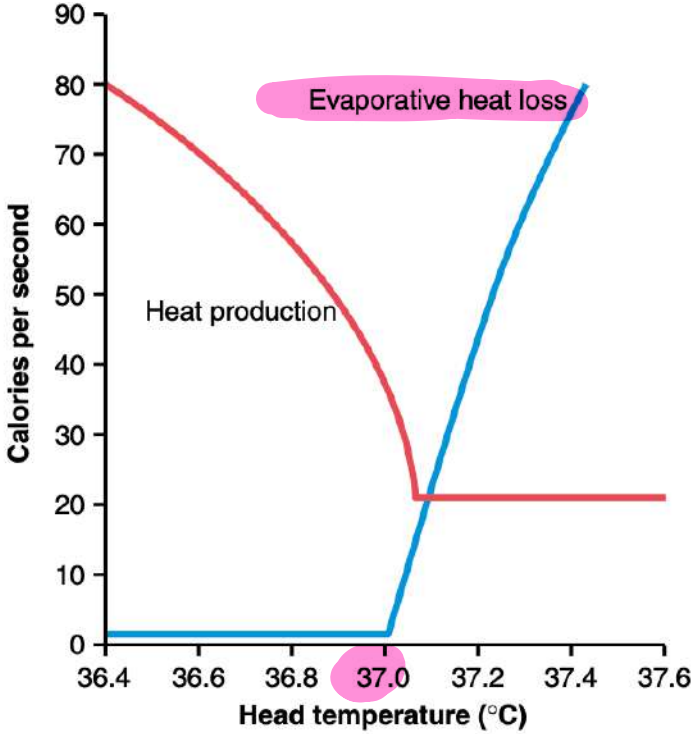

Figure 73-7 Effect of hypothalamic temperature on evaporative heat loss from the body and on heat production caused primarily by muscle activity and shivering. This figure demonstrates the extremely critical temperature level at which increased heat loss begins and heat production reaches a minimum stable level.

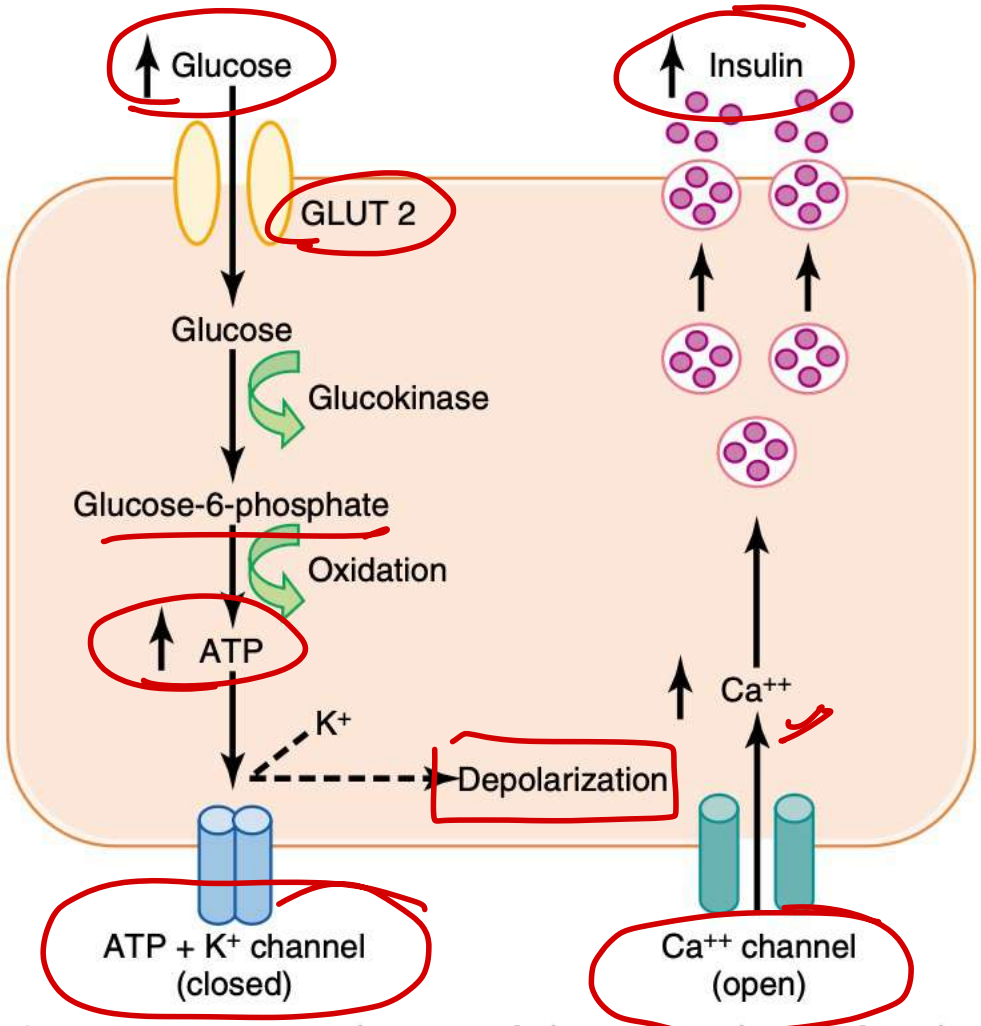

Figure 78-7 Basic mechanisms of glucose stimulation of insulin secretion by beta cells of the pancreas. GLUT, glucose transporter.

Increase Insulin Secretion	Decrease Insulin Secretion
Increased blood glucose	Decreased blood glucose
Increased blood free fatty acids	Fasting
Increased blood amino acids	Somatostatin
Gastrointestinal hormones (gastrin, cholecystokinin, secretin, gastric inhibitory peptide)	α-Adrenergic activity
Glucagon, growth hormone, cortisol	Leptin
Parasympathetic stimulation; acetylcholine	
β-Adrenergic stimulation	
Insulin resistance; obesity	
Sulfonylurea drugs (glyburide, tolbutamide)	

Feature	Type I	Type II
Age at onset	Usually <20 yr	Usually >30 yr
Body mass	Low (wasted) to Normal	Obese
Plasma insulin	Low or absent	Normal to high initially
Plasma glucagon	High, can be suppressed	High, resistant to suppression
Plasma glucose	Increased	Increased
Insulin sensitivity	Normal	Reduced
Therapy	Insulin	Weight loss, thiazolidinediones, metformin, sulfonylureas, insulin

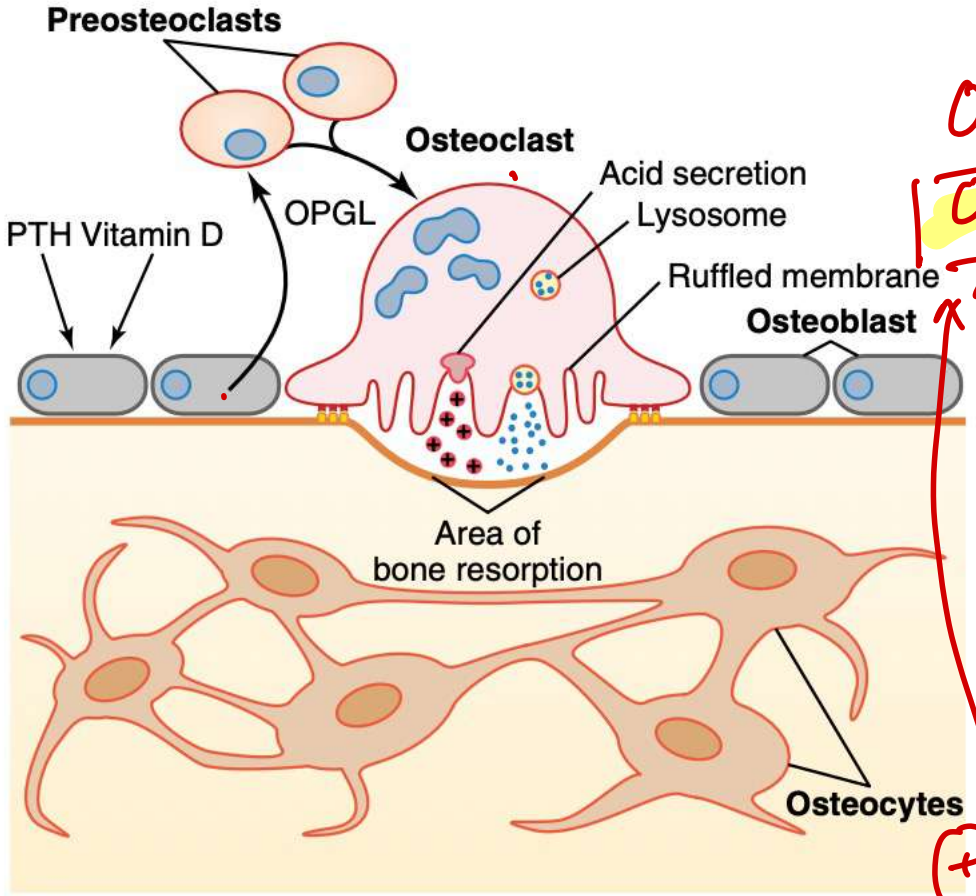

Figure 79-5 Bone resorption by osteoclasts. Parathyroid hormone (PTH) binds to receptors on osteoblasts, causing them to release osteoprotegerin ligand (OPGL), which binds to receptors on preosteoclast cells. This causes the cells to differentiate into mature osteoclasts. The osteoclasts then develop a ruffled border and release enzymes from lysosomes, as well as acids that promote bone resorption. Osteocytes are osteoblasts that have become encased in bone matrix during bone tissue production; the osteocytes form a system of interconnected cells that spreads all through the bone.

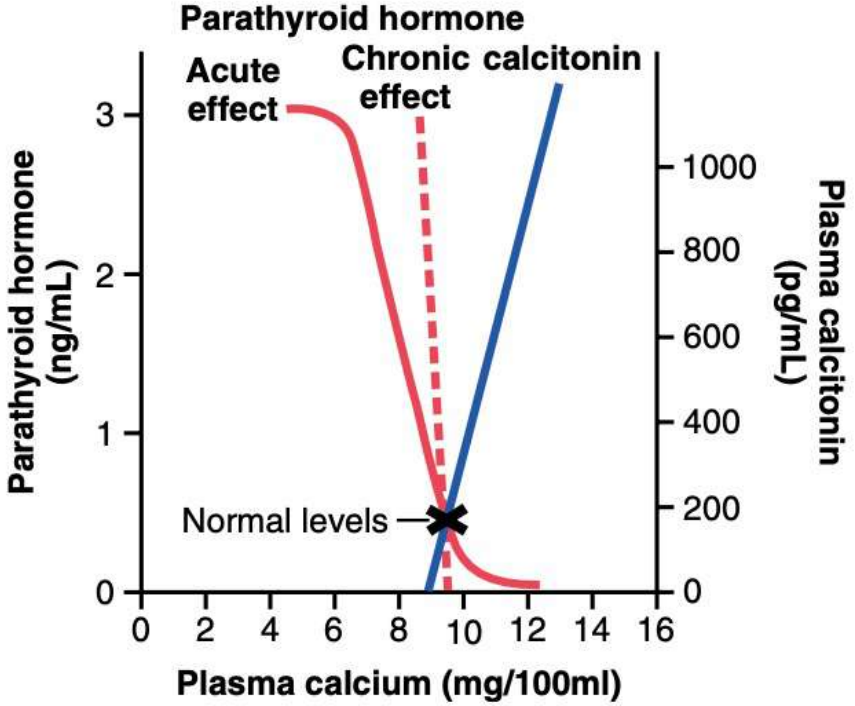

Figure 79-12 Approximate effect of plasma calcium concentration on the plasma concentrations of parathyroid hormone and calcitonin. Note especially that long-term, chronic changes in calcium concentration of only a few percentage points can cause as much as 100 percent change in parathyroid hormone concentration.

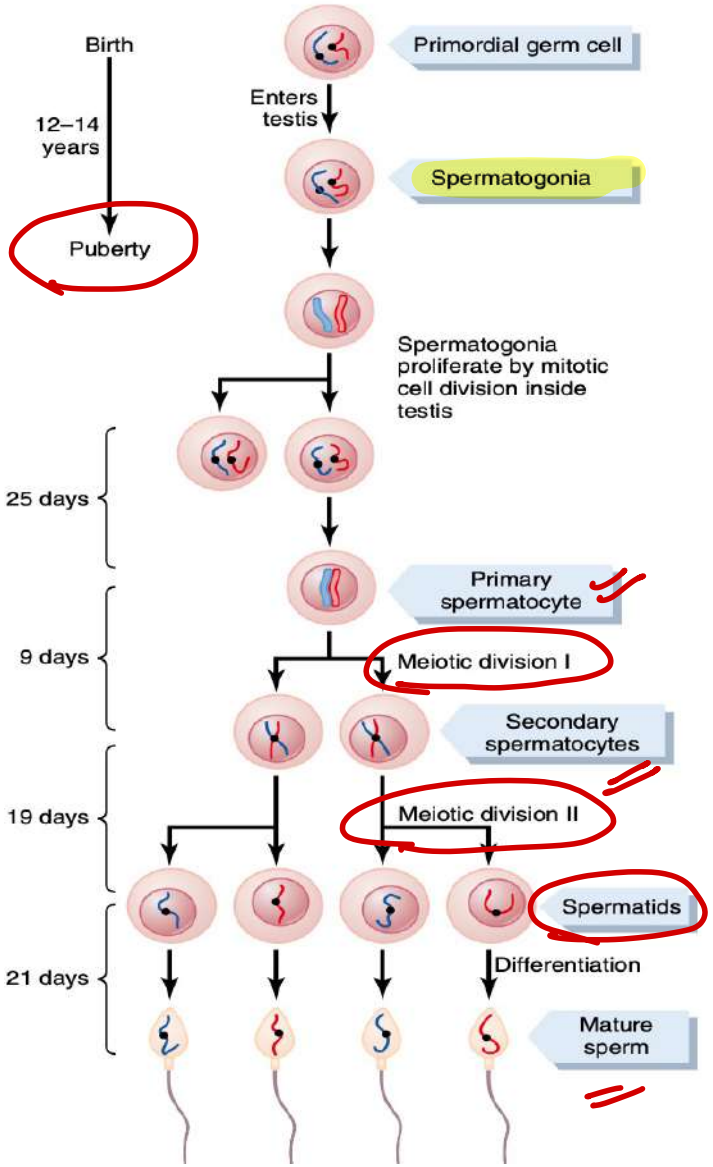

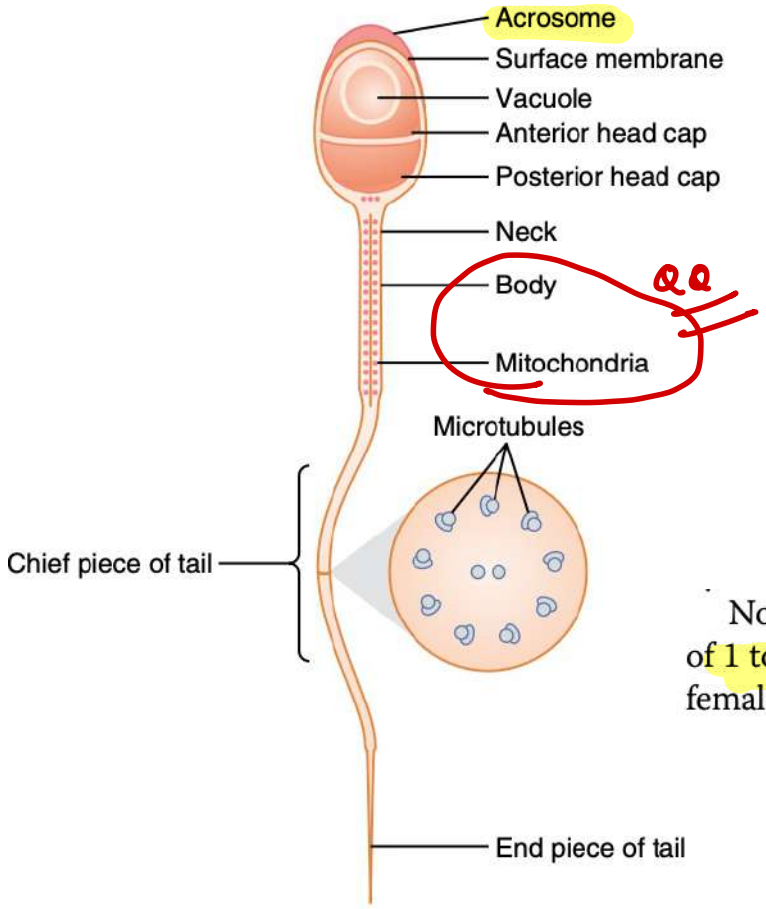

Figure 80-4 Structure of the human spermatozoon.

Stored in the acrosome of the sperm are large quantities of *hyaluronidase* and *proteolytic enzymes*. Hyaluronidase depolymerizes the hyaluronic acid polymers in the intercellular cement that holds the ovarian granulosa cells together. The proteolytic enzymes digest proteins in the structural elements of tissue cells that still adhere to the ovum.

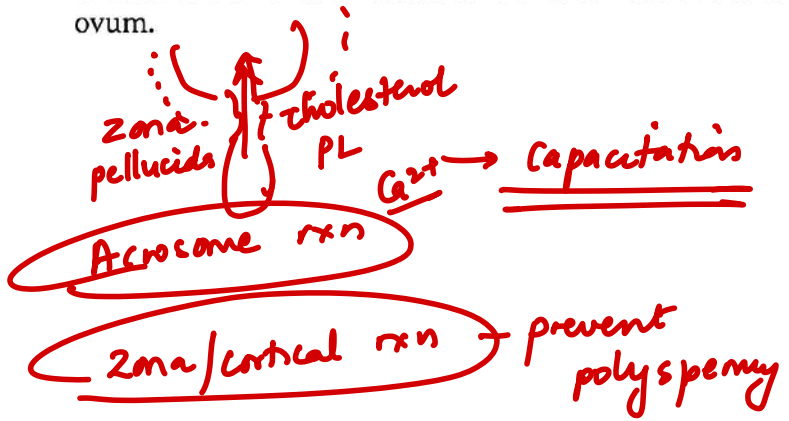

Normal sperm move in a fluid medium at a velocity of 1 to 4 mm/min. This allows them to move through the female genital tract in quest of the ovum.

↑ locomn

SEMINAL VESICLE: fructose / citric acid / PG / fibrinogen
PROSTATE: Ca^{2+} / clotting factors → alkaline
CAPACITATION-7-10hrs — Cholesterol released

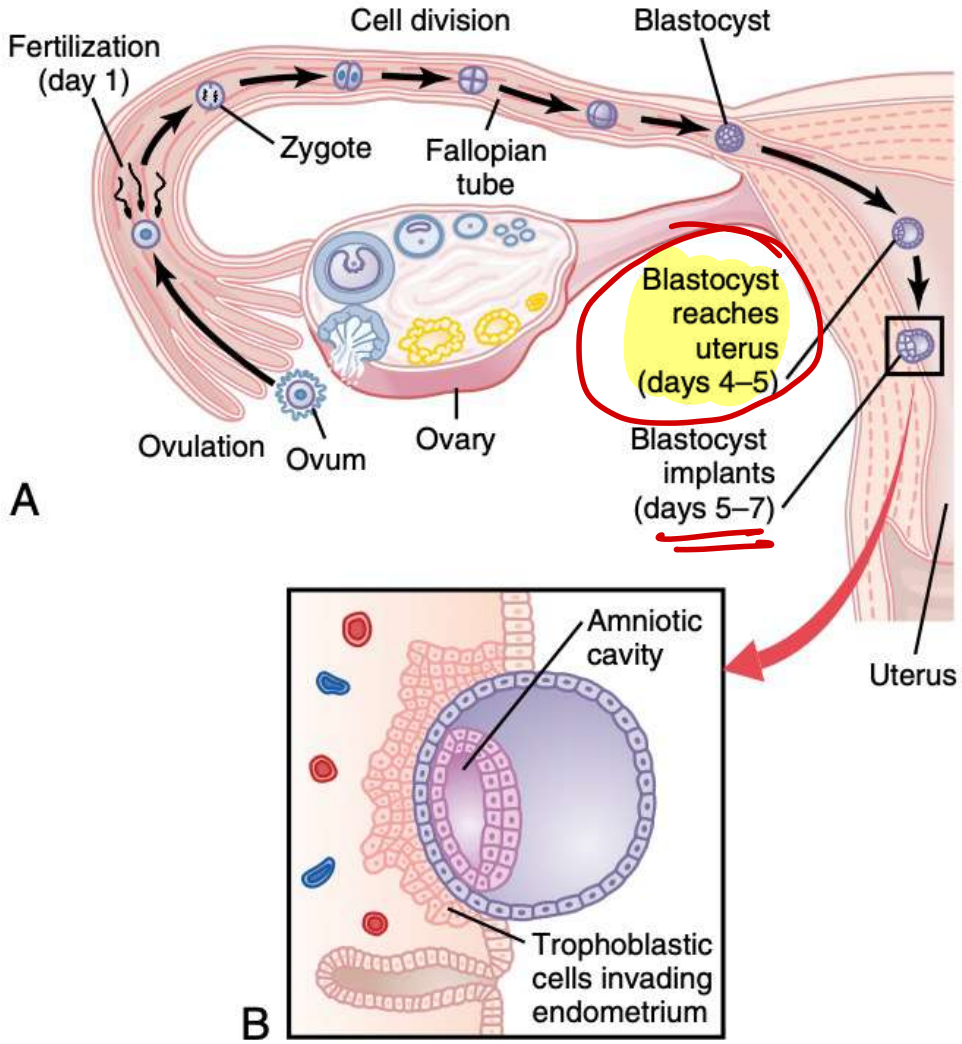

Figure 82-2 *A,* Ovulation, fertilization of the ovum in the fallopian tube, and implantation of the blastocyst in the uterus. *B,* Action of trophoblast cells in implantation of the blastocyst in the uterine endometrium.

Meiosis -2

Once a sperm has entered the ovum (which is still in the secondary oocyte stage of development), the oocyte divides again to form the *mature ovum* plus a *second polar body* that is expelled. The mature ovum still carries in its nucleus (now called the *female pronucleus*) 23 chromosomes. One of these chromosomes is the female chromosome, known as the *X chromosome.*

In the meantime, the fertilizing sperm has also changed. On entering the ovum, its head swells to form a *male pronucleus,* shown in Figure 82-1*D*. Later, the 23 unpaired chromosomes of the male pronucleus and the 23 unpaired chromosomes of the female pronucleus align themselves

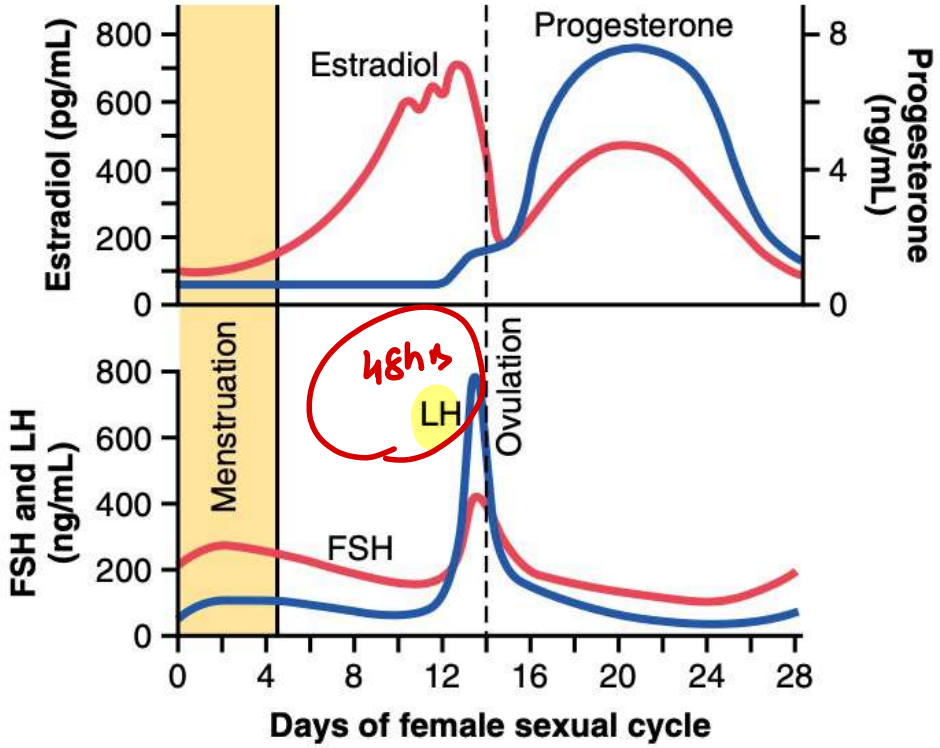

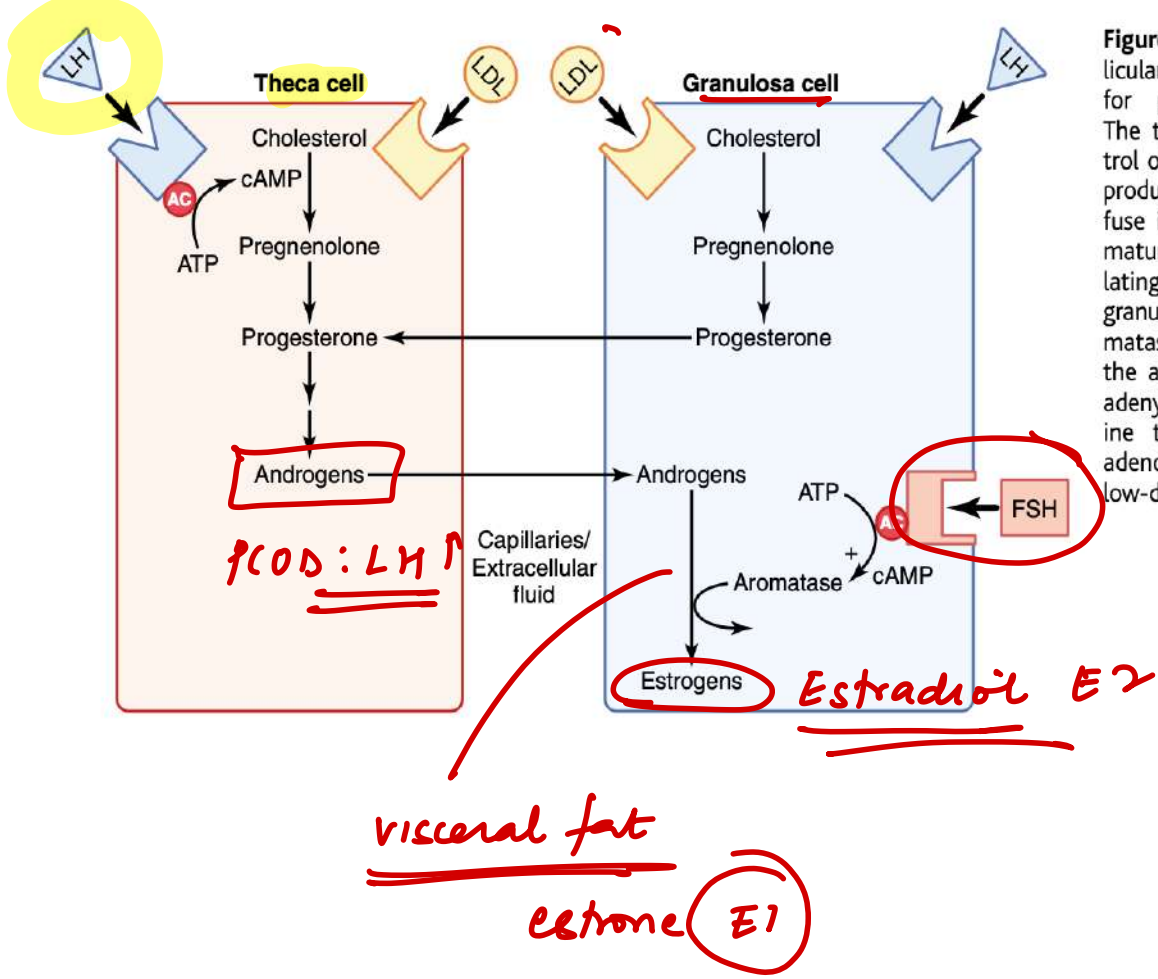

Figure 81-7 Interaction of follicular theca and granulosa cells for production of estrogens. The theca cells, under the control of luteinizing hormone (LH), produce androgens that diffuse into the granulosa cells. In mature follicles, follicle stimulating hormone (FSH) acts on granulosa cells to stimulate aromatase activity, which converts the androgens to estrogens. AC, adenylate cyclase; ATP, adenosine triphosphate; cAMP, cyclic adenosine monophosphate; LDL, low-density lipoproteins.

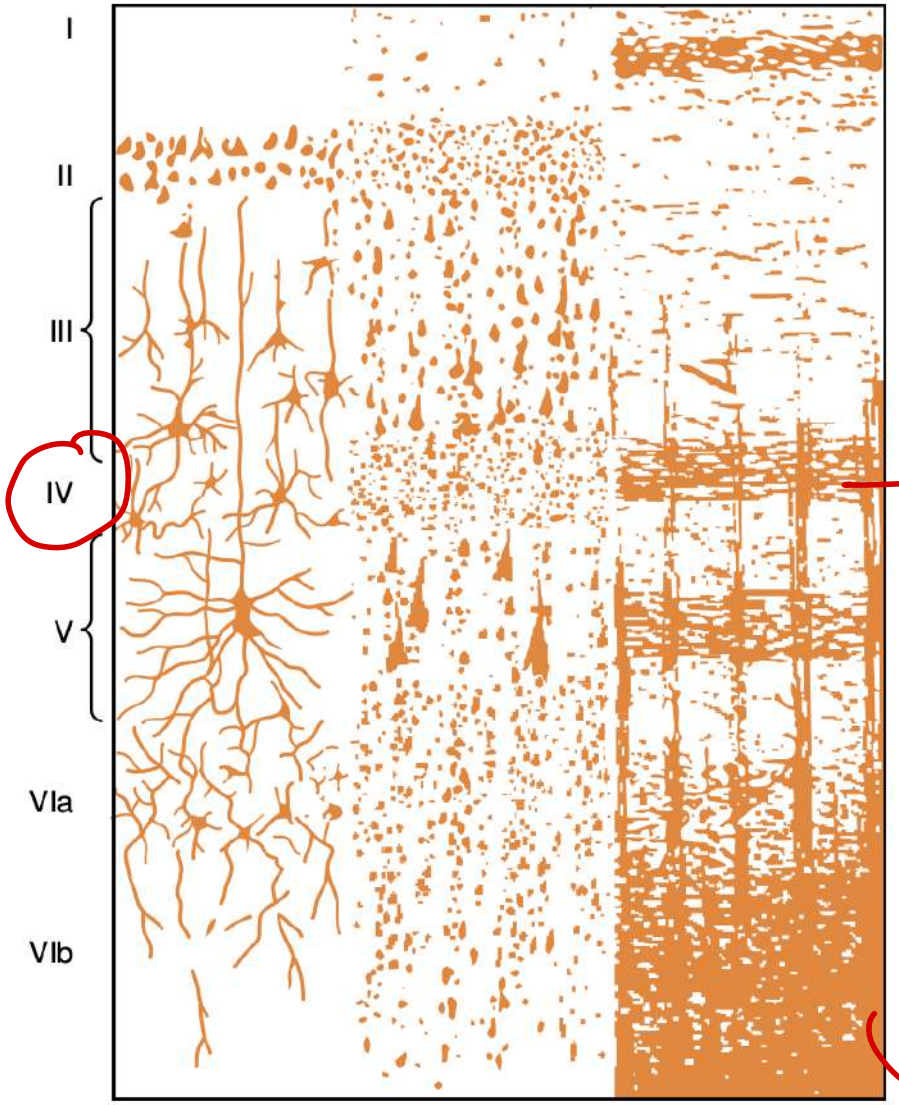

Figure 57-1 Structure of the cerebral cortex, showing: *I*, molecular layer; *II*, external granular layer; *III*, layer of pyramidal cells; *IV*, internal granular layer; *V*, large pyramidal cell layer; and *VI*, layer of fusiform or polymorphic cells. (Redrawn from Ranson SW, Clark SL [after Brodmann]: Anatomy of the Nervous System. Philadelphia: WB Saunders, 1959.)

I/II/III – associations

IV → incoming fibres

V/VI → output

thalamus

basal ganglia

granular

fusiform

pyramidal

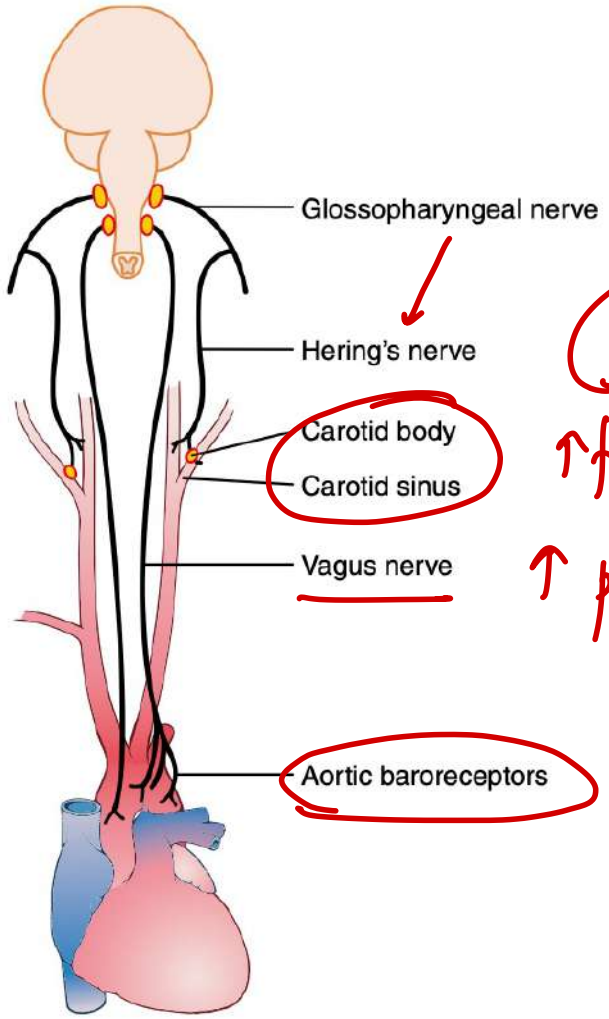

Figure 18-5 The baroreceptor system for controlling arterial pressure.

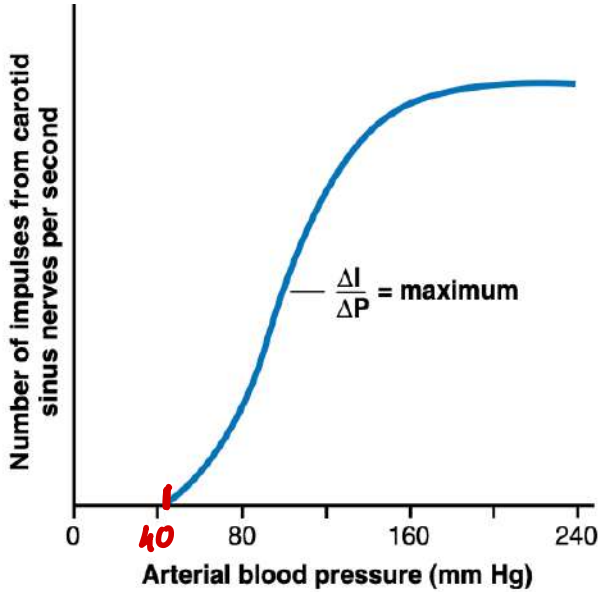

igure 18-6 Activation of the baroreceptors at different levels of rterial pressure. ΔI, change in carotid sinus nerve impulses per econd; ΔP, change in arterial blood pressure in mm Hg.

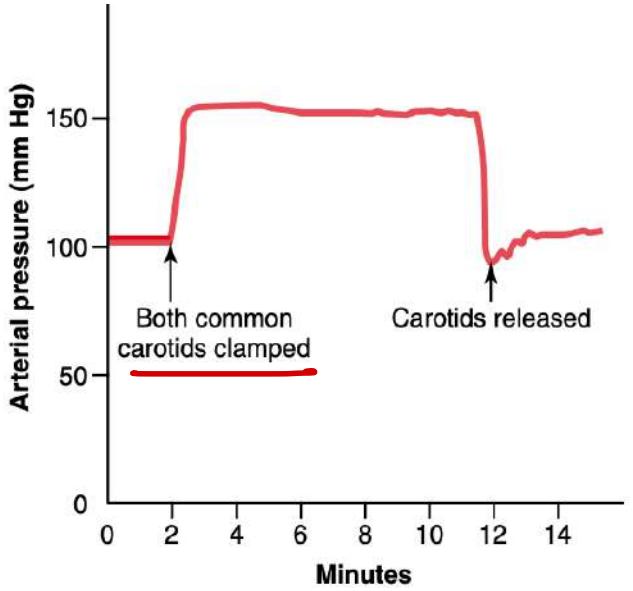

Figure 18-7 Typical carotid sinus reflex effect on aortic arterial pressure caused by clamping both common carotids (after the two vagus nerves have been cut).

Physiologic Anatomy of the Baroreceptors and Their Innervation. Baroreceptors are spray-type nerve endings that lie in the walls of the arteries; they are stimulated when stretched. A few baroreceptors are located in the wall of almost every large artery of the thoracic and neck regions; but, as shown in Figure 18-5, baroreceptors are extremely abundant in (1) the wall of each internal carotid artery slightly above the carotid bifurcation, an area known as the *carotid sinus,* and (2) the wall of the aortic arch.

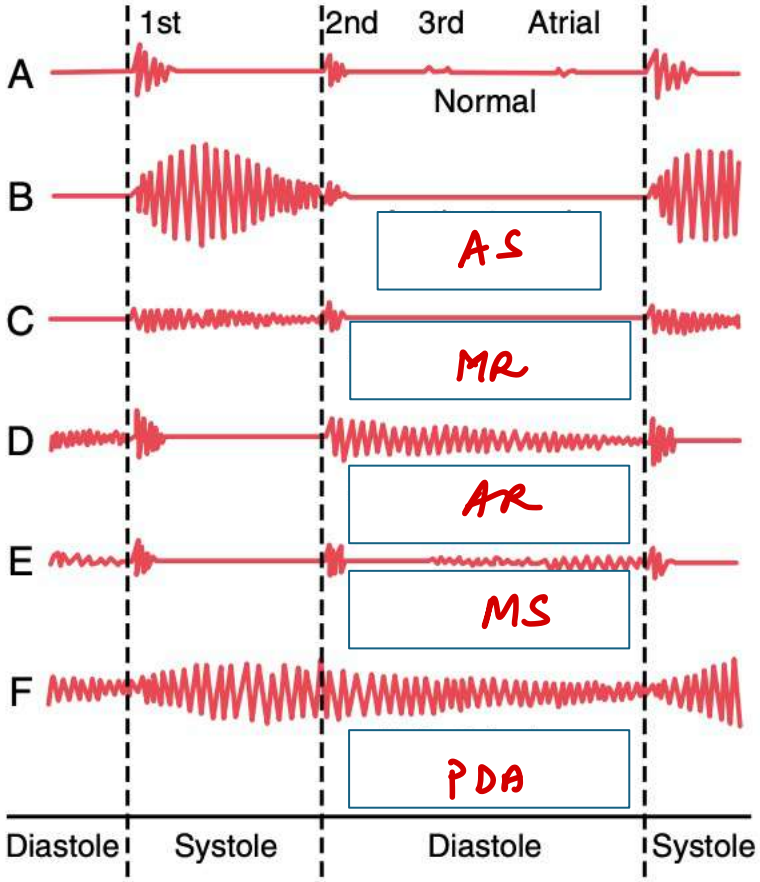

Figure 23-3 Phonocardiograms from normal and abnormal hearts.

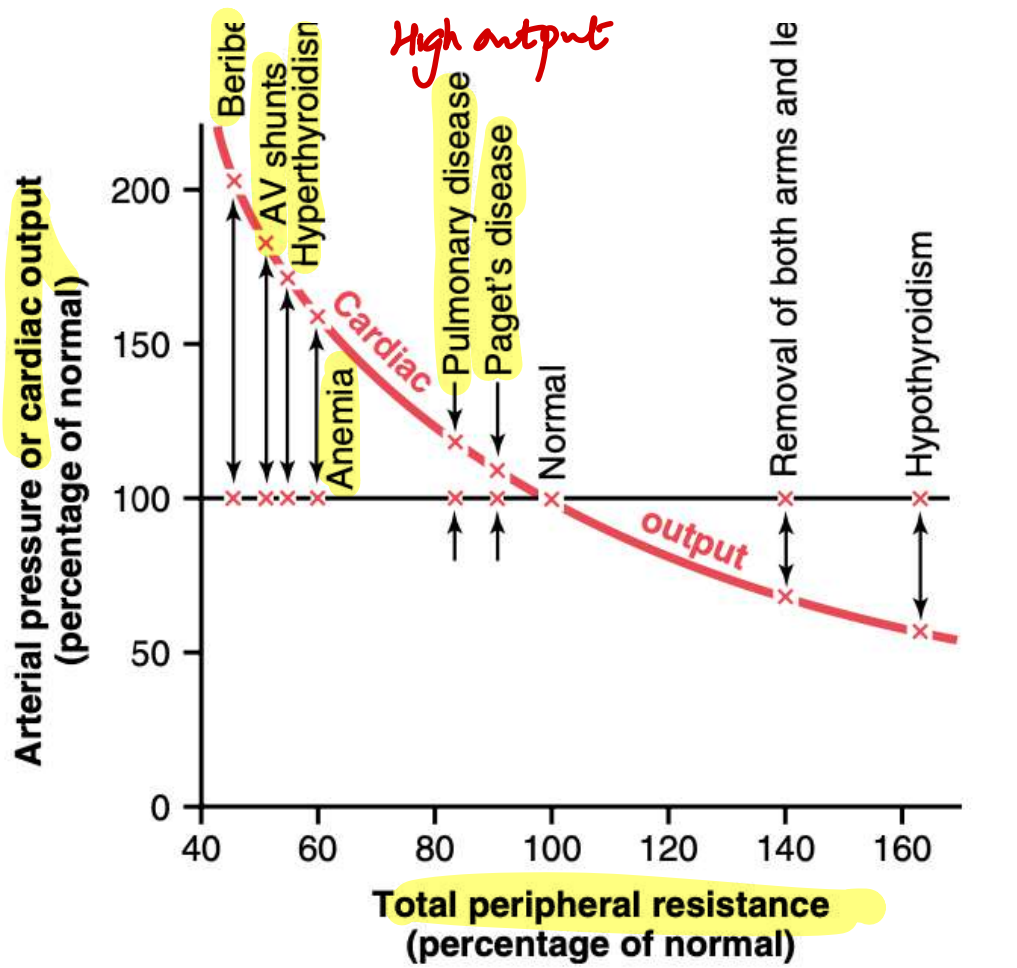

Figure 20-3 Chronic effect of different levels of total peripheral resistance on cardiac output, showing a reciprocal relationship between total peripheral resistance and cardiac output. (Redrawn from Guyton AC: Arterial Pressure and Hypertension. Philadelphia: WB Saunders, 1980.)

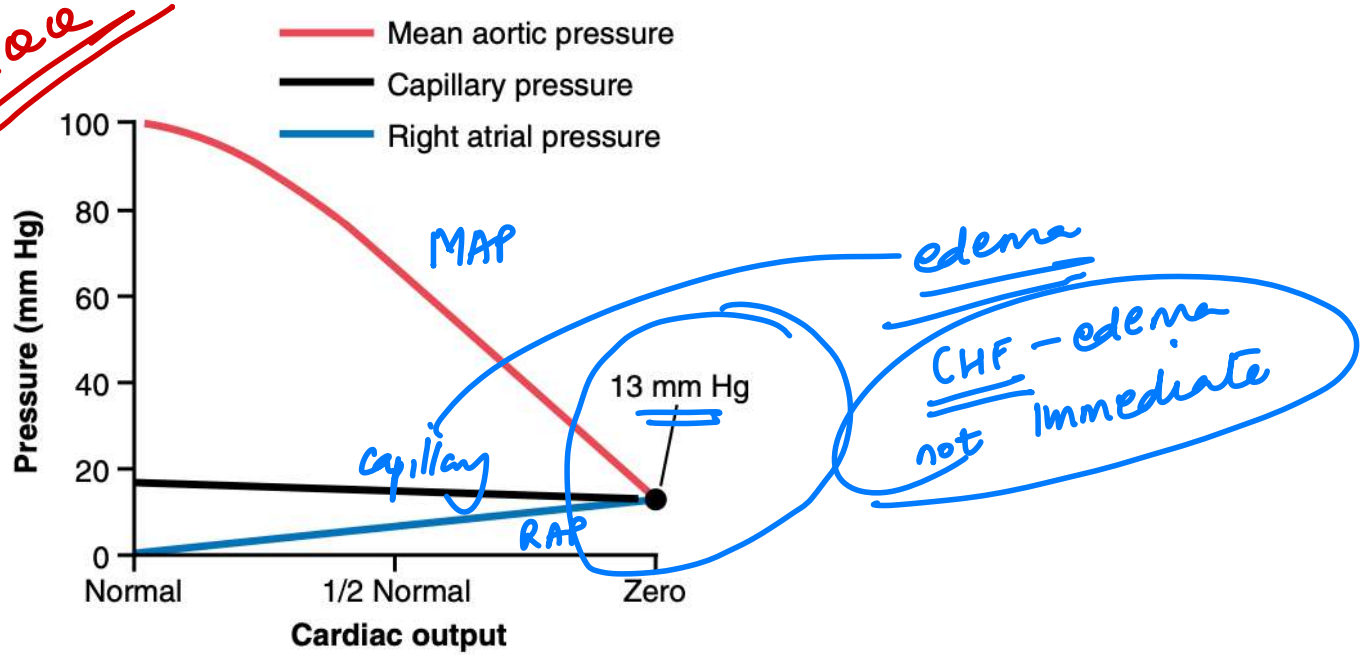

Figure 22-3 Progressive changes in mean aortic pressure, peripheral tissue capillary pressure, and right atrial pressure as the cardiac output falls from normal to zero.

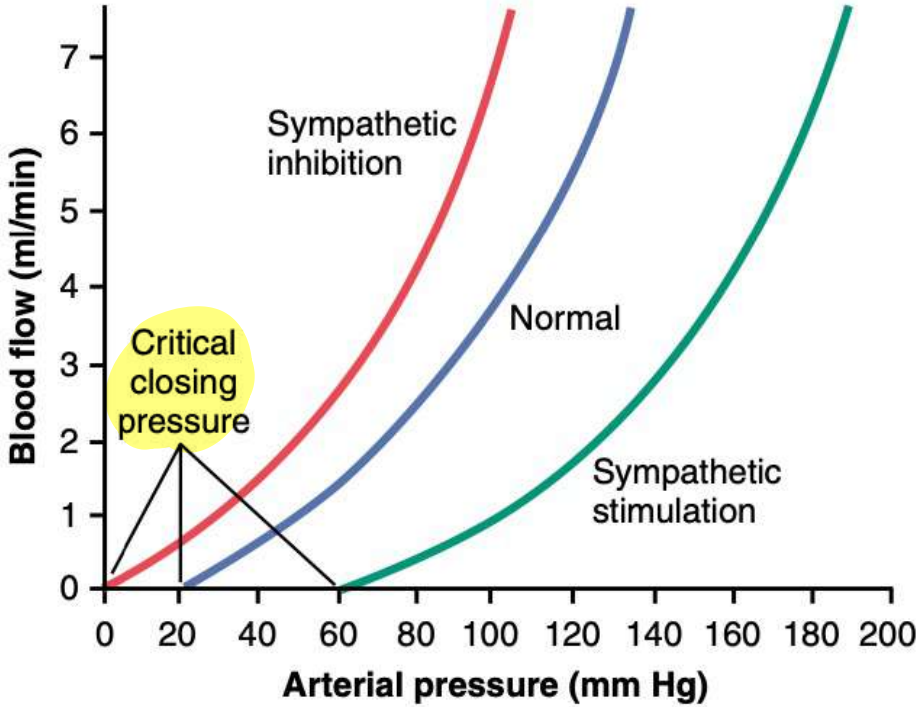

Figure 14-13 Effect of arterial pressure on blood flow through a *passive* blood vessel at different degrees of vascular tone caused by increased or decreased sympathetic stimulation of the vessel.

Capillary pressure also falls from its normal value o
17 mm Hg to the new equilibrium pressure of 13 mn
Hg. Thus, *severe acute cardiac failure often causes a*
fall in peripheral capillary pressure rather than a rise
Therefore, animal experiments, as well as experience in
humans, show that acute cardiac failure almost neve
causes immediate development of peripheral edema.

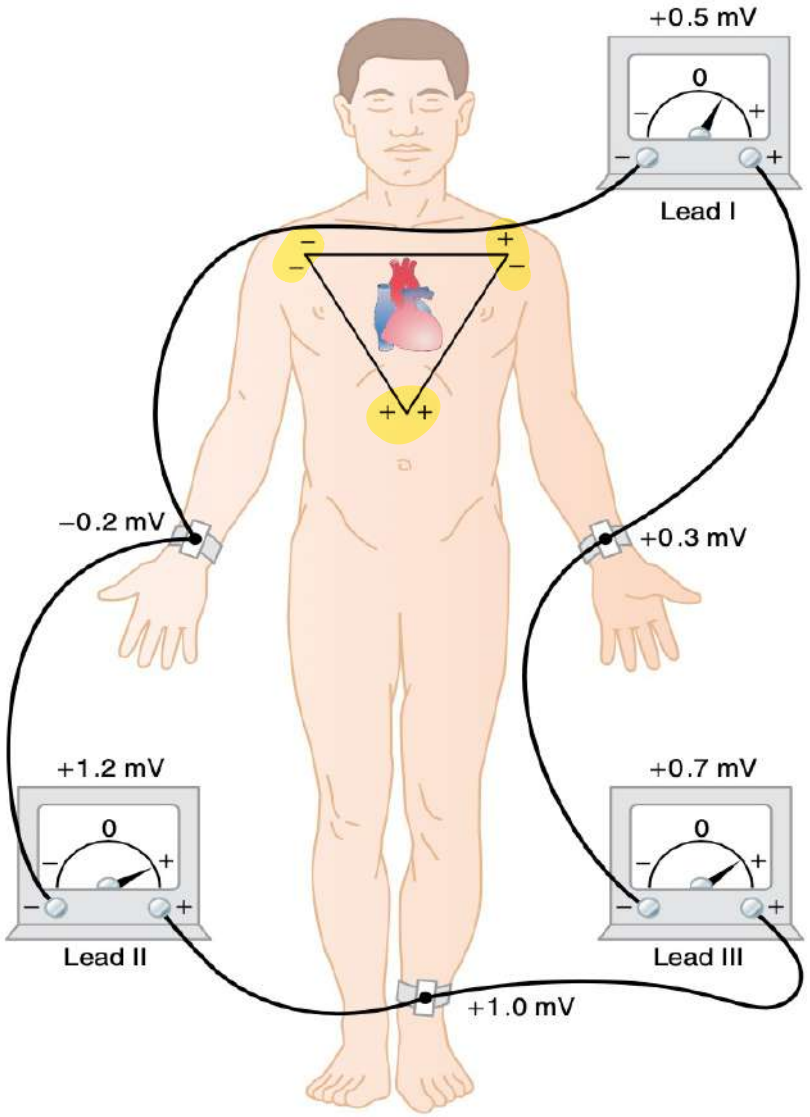

Einthoven's law

1 + 3 = 2

Now, note that the sum of the voltages in leads I and III equals the voltage in lead II; that is, 0.5 plus 0.7 equals 1.2. Mathematically, this principle, called Einthoven's law, holds true at any given instant while the three "standard" bipolar electrocardiograms are being recorded.

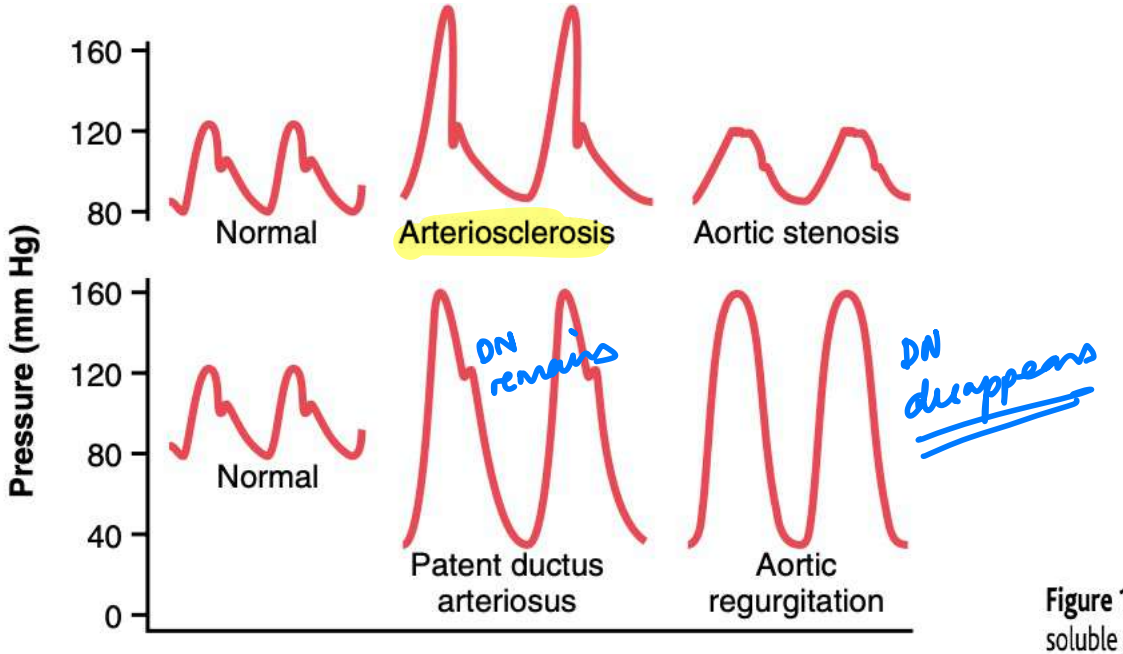

Figure 15-4 Aortic pressure pulse contours in arteriosclerosis, aortic stenosis, patent ductus arteriosus, and aortic regurgitation.

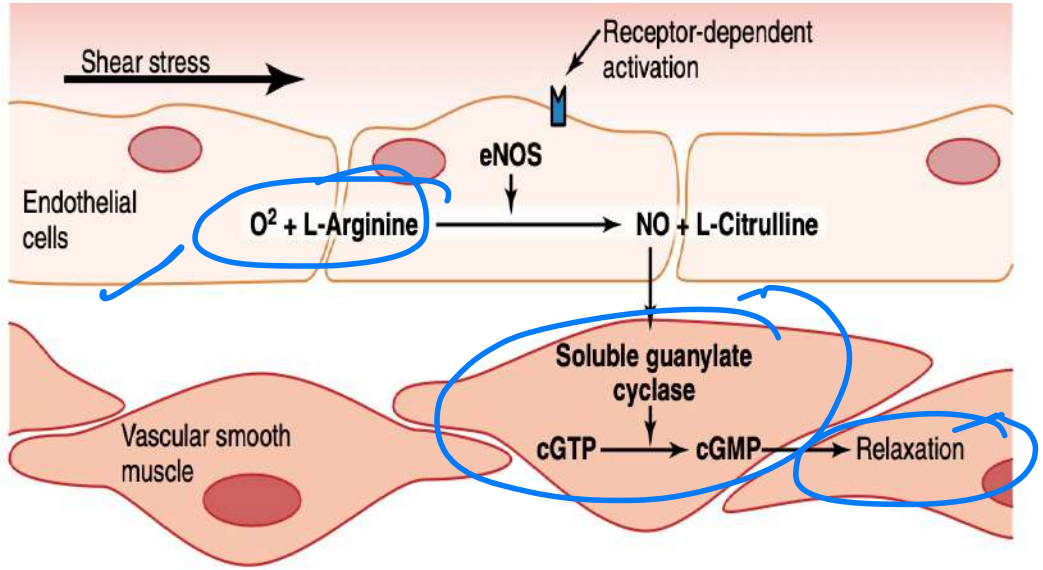

Figure 17-5 Nitric oxide synthase (eNOS) enzyme in endothelial cells synthesizes nitric oxide (NO) from arginine and oxygen. NO activates soluble guanylate cyclases in vascular smooth muscle cells, resulting in conversion of cyclic guanosine triphosphate (cGTP) to cyclic guanosine monophosphate (cGMP) which ultimately causes the blood vessels to relax.

NO = EDRF – iNO – PAH

arginine

cGMP ↑

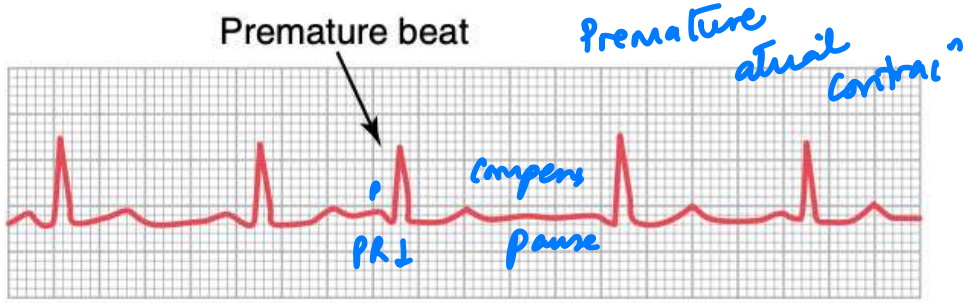

Symptoms of Decompression Sickness ("Bends"). The symptoms of decompression sickness are caused by gas bubbles blocking many blood vessels in different tissues. At first, only the smallest vessels are blocked by minute bubbles, but as the bubbles coalesce, progressively larger vessels are affected. Tissue ischemia and sometimes tissue death result.

In most people with decompression sickness, the symptoms are pain in the joints and muscles of the legs and arms, affecting 85 to 90 percent of those persons who develop decompression sickness. The joint pain accounts for the term "bends" that is often applied to this condition.

In 5 to 10 percent of people with decompression sickness, nervous system symptoms occur, ranging from dizziness in about 5 percent to paralysis or collapse and unconsciousness in as many as 3 percent. The paralysis may be temporary, but in some instances, damage is permanent.

Finally, about 2 percent of people with decompression sickness develop "the chokes," caused by massive numbers of microbubbles plugging the capillaries of the lungs; this is characterized by serious shortness of breath, often followed by severe pulmonary edema and, occasionally, death.

The observed effects of prolonged stay in space are the following: (1) decrease in blood volume, (2) decrease in red blood cell mass, (3) decrease in muscle strength and work capacity, (4) decrease in maximum cardiac output, and (5) loss of calcium and phosphate from the bones, as well as loss of bone mass. Most of these same effects also occur in people who lie in bed for an extended period of time. For this reason, exercise programs are carried out by astronauts during prolonged space missions.

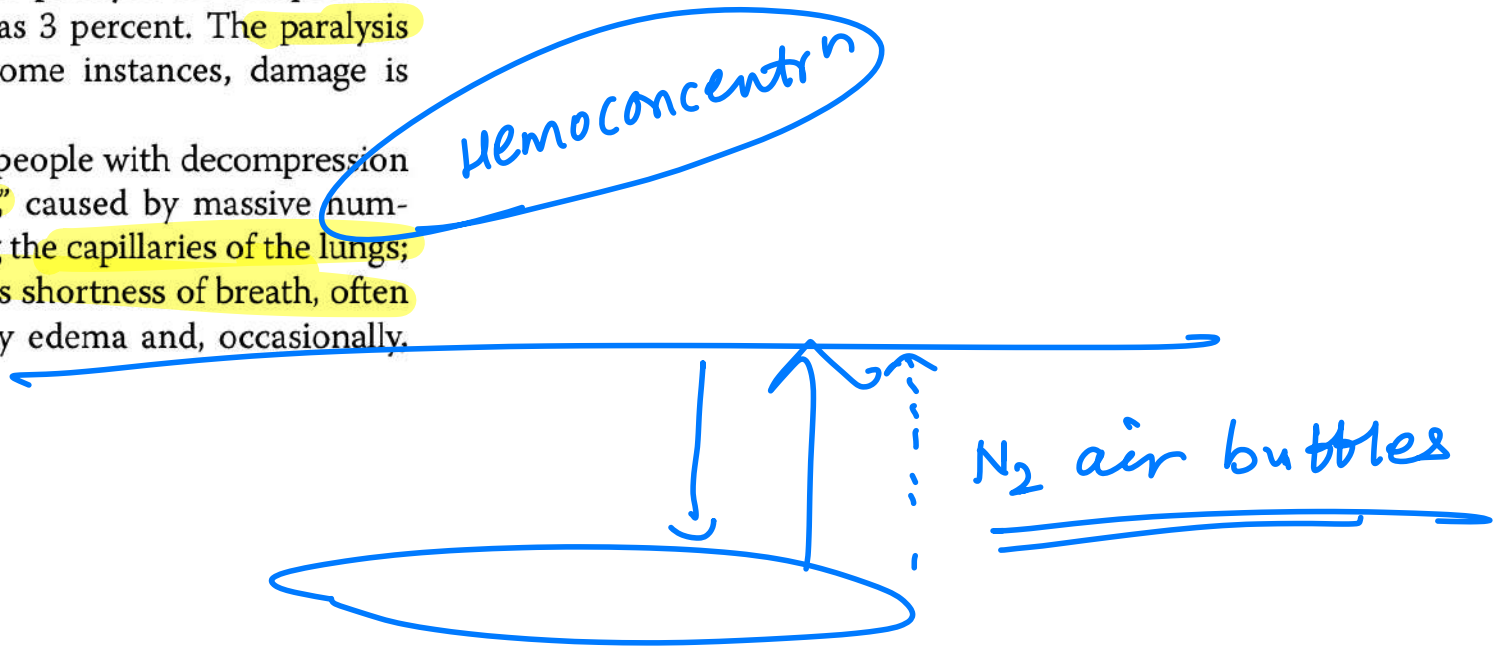

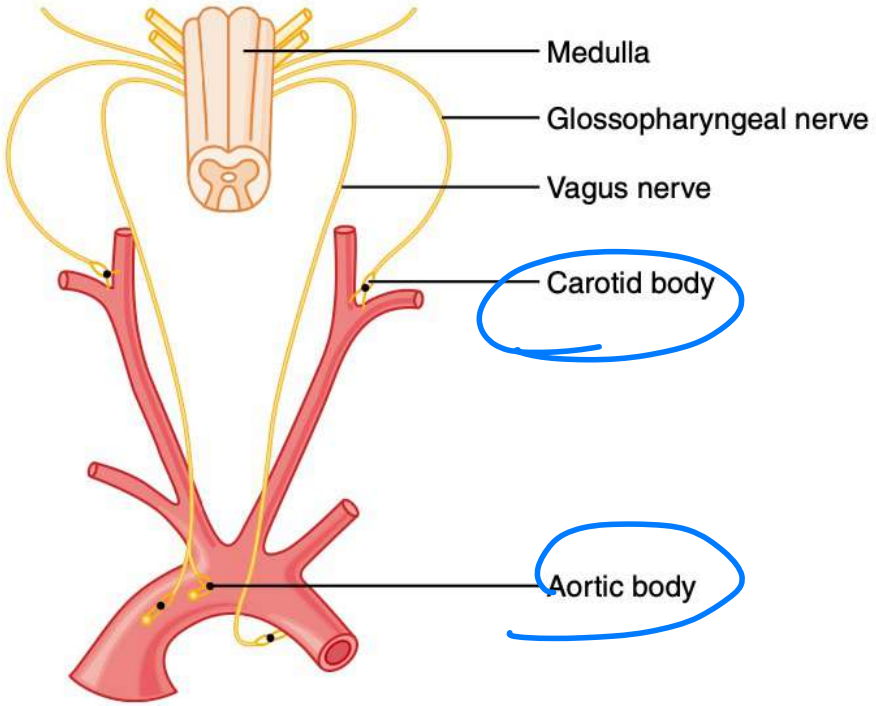

Chemoreceptor

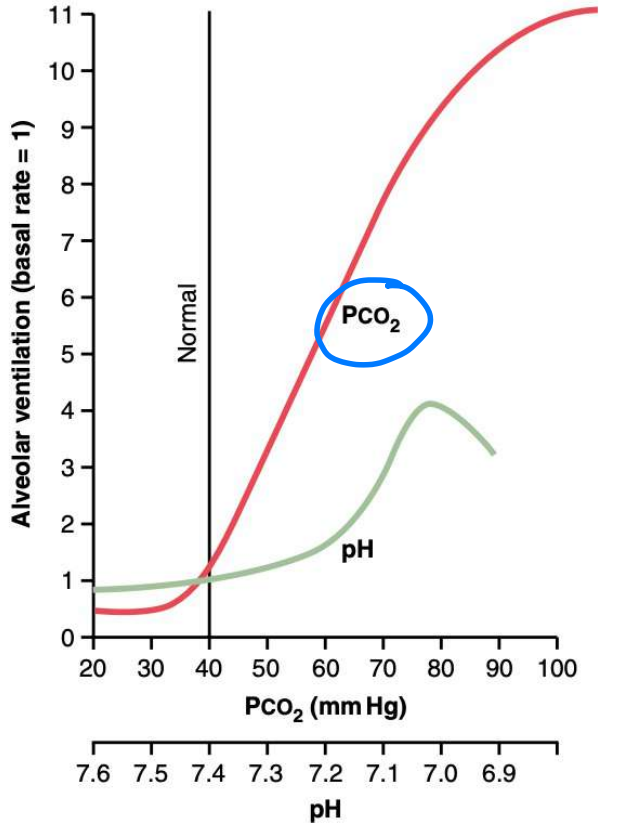

Figure 41-3 Effects of increased arterial blood P_{CO_2} and decreas arterial pH (increased hydrogen ion concentration) on the rate alveolar ventilation.

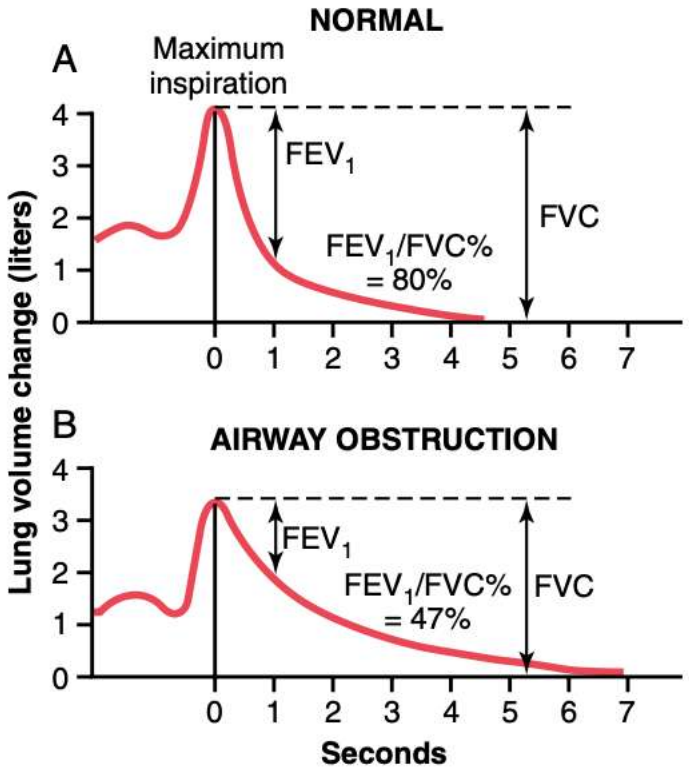

Figure 42-3 Recordings during the forced vital capacity maneuver: *A*, in a healthy person and *B*, in a person with partial airway obstruction. (The "zero" on the volume scale is residual volume.)

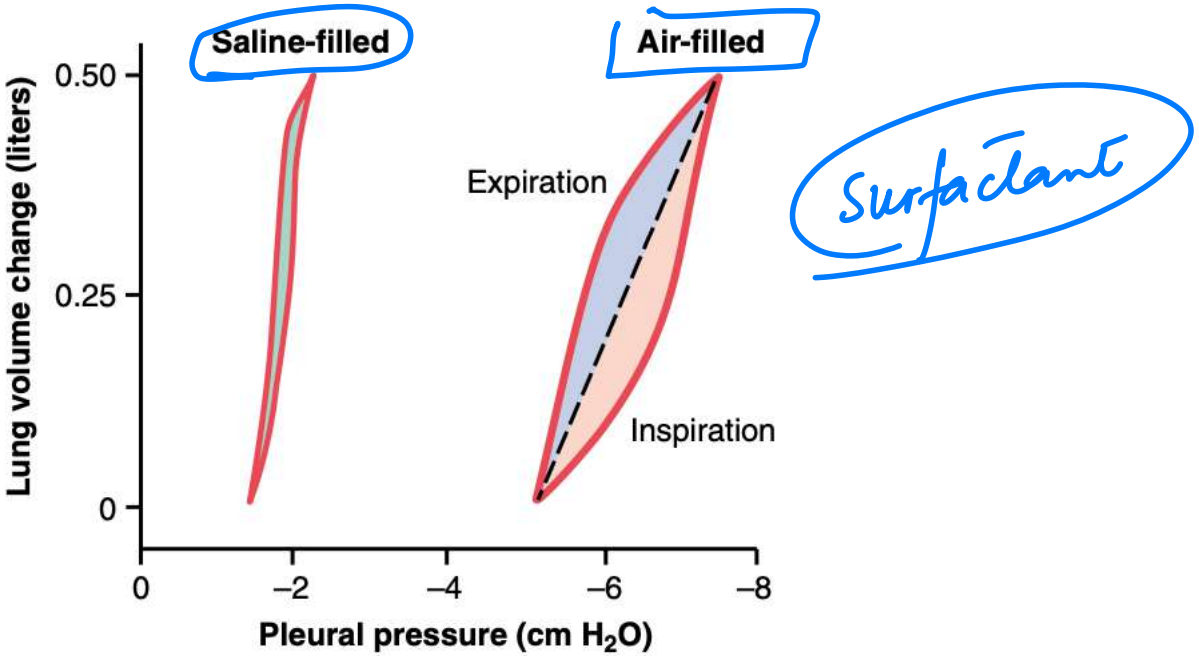

Figure 37-4 Comparison of the compliance diagrams of saline-filled and air-filled lungs when the alveolar pressure is maintained at atmospheric pressure (0 cm H_2O) and pleural pressure is changed.

can conclude that *the tissue elastic forces tending to cause collapse of the air-filled lung represent only about one third of the total lung elasticity, whereas the fluid-air surface tension forces in the alveoli represent about two thirds.*

The fluid-air surface tension elastic forces of the lungs also increase tremendously when the substance called *surfactant* is *not* present in the alveolar fluid. Let us now

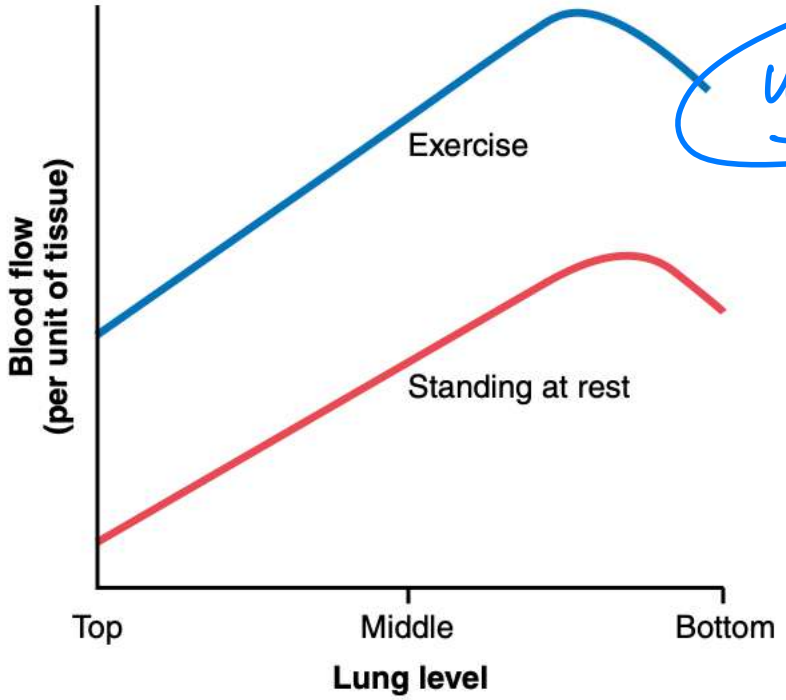

uniform Q ↑↑

all zones ↑

Figure 38-3 Blood flow at different levels in the lung of an upright person *at rest* and *during exercise*. Note that when the person is at rest, the blood flow is very low at the top of the lungs; most of the flow is through the bottom of the lung.

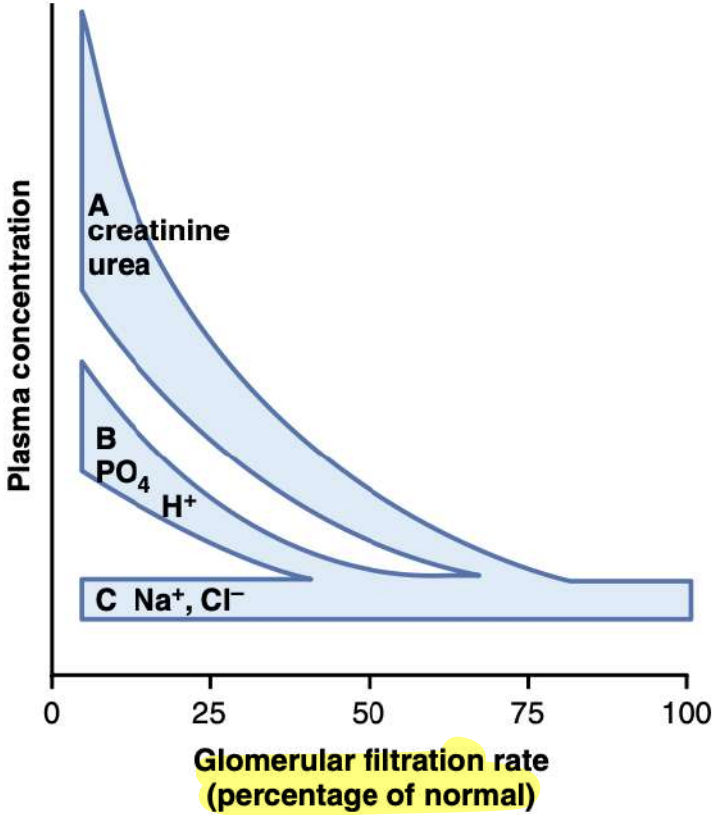

Figure 31-5 Representative patterns of adaptation for different types of solutes in chronic renal failure. Curve A shows the approximate changes in the plasma concentrations of solutes such as creatinine and urea that are filtered and poorly reabsorbed. Curve B shows the approximate concentrations for solutes such as phosphate, urate, and hydrogen ion. Curve C shows the approximate concentrations for solutes such as sodium and chloride.

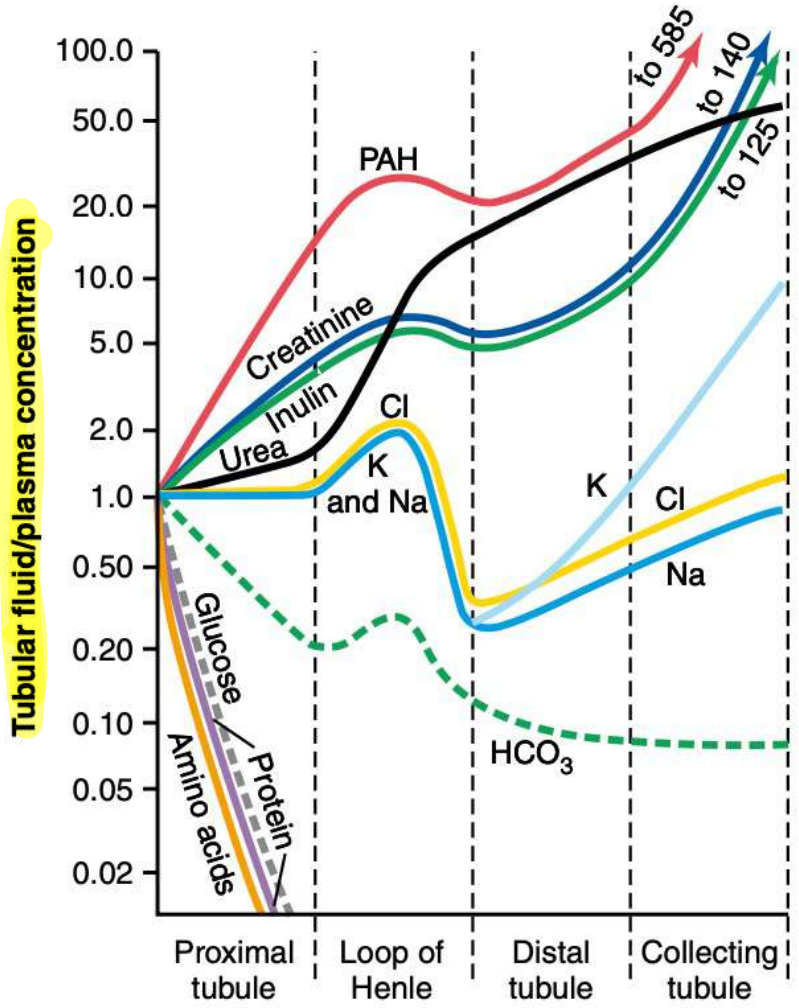

Figure 27-14 Changes in average concentrations of different substances at different points in the tubular system relative to the concentration of that substance in the plasma and in the glomerular filtrate. A value of 1.0 indicates that the concentration of the substance in the tubular fluid is the same as the concentration of that substance in the plasma. Values below 1.0 indicate that the substance is reabsorbed more avidly than water, whereas values above 1.0 indicate that the substance is reabsorbed to a lesser extent than water or is secreted into the tubules.

$\frac{TF}{P} = 1$ isotonic

$TF/P > 1$ ↳ secretion

$TF/P < 1$ ↳ reabsorp

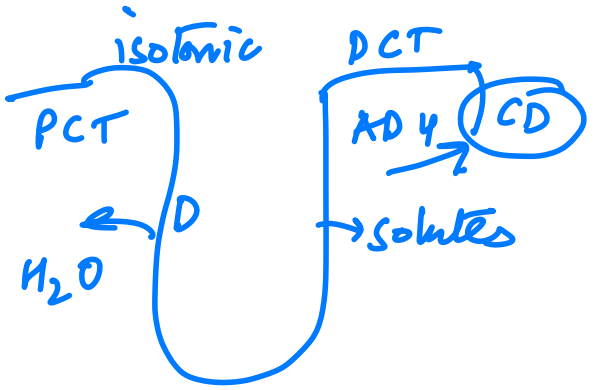

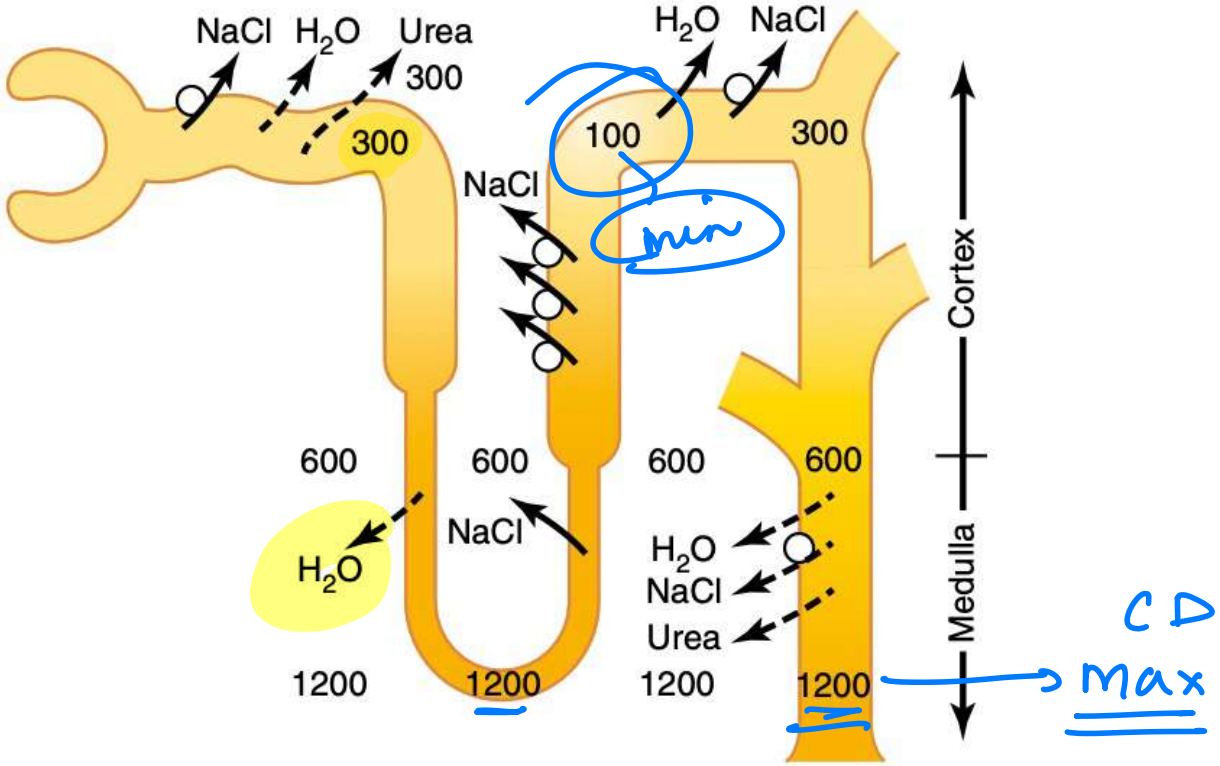

Figure 28-5 Formation of a concentrated urine when antidiuretic hormone (ADH) levels are high. Note that the fluid leaving the loop of Henle is dilute but becomes concentrated as water is absorbed from the distal tubules and collecting tubules. With high ADH levels, the osmolarity of the urine is about the same as the osmolarity of the renal medullary interstitial fluid in the papilla, which is about 1200 mOsm/L. (Numerical values are in milliosmoles per liter.)

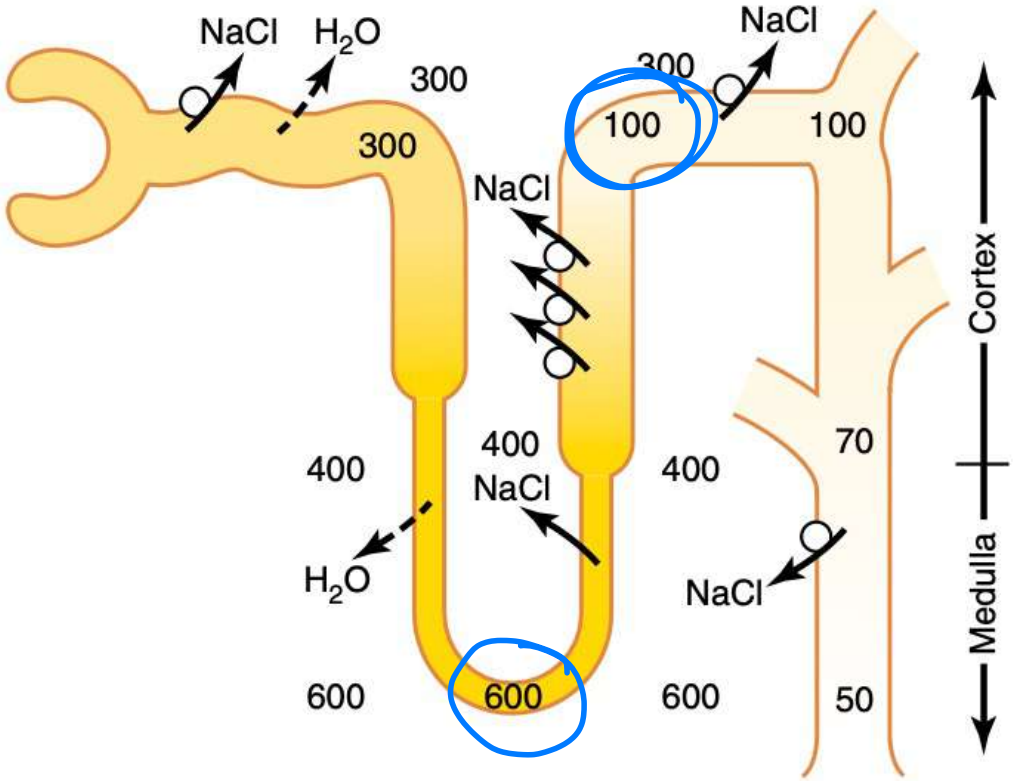

Figure 28-2 Formation of dilute urine when antidiuretic hormone (ADH) levels are very low. Note that in the ascending loop of Henle, the tubular fluid becomes very dilute. In the distal tubules and collecting tubules, the tubular fluid is further diluted by the reabsorption of sodium chloride and the failure to reabsorb water when ADH levels are very low. The failure to reabsorb water and continued reabsorption of solutes lead to a large volume of dilute urine. (Numerical values are in milliosmoles per liter.)